Increased lymphocyte apoptosis in mouse models of colitis upon ABT-737 treatment is dependent upon BIM expression

Lutz, C ; Mozaffari, M ; Tosevski, V ; Caj, M ; Cippà, P ; McRae, B L ; Graff, C L ; Rogler, G ; Fried, M ; Hausmann, M

Abstract: Exaggerated activation of lymphocytes contributes to the pathogenesis of inflammatory bowel disease (IBD). Medical therapies are linked to the BCL-2 family-mediated apoptosis. Imbalance in BCL-2 family proteins may cause failure in therapeutic responses. We investigated the role of BCL-2 inhibitor ABT-737 for lymphocyte apoptosis in mice under inflammatory conditions. B.6129P2-interleukin (IL)-10(tm1Cgn) /J (IL-10(-/-)) weighing 25-30 g with ongoing colitis were used. Fifty mg/kg/day ABT-737 was injected intraperitoneally (i.p.). Haematological analyses were performed with an ADVIA 2120 flow cytometer and mass cytometry with a CyTOF 2. Following i.p. administration, ABT-737 was detected in both spontaneous and acute colitis in peripheral blood (PBL) and colon tissue. Treatment led to lymphopenia. CD4(+) CD44(+) CD62L(+) central memory and CD8(+) , CD44(+) CD62L(-) central memory T cells were decreased in PBL upon ABT-737 compared to vehicle-receiving controls. Increased apoptosis upon ABT-737 was determined in blood lymphocytes, splenocytes and Peyer's patches and was accompanied by a decrease in TNF and IL-1B. ABT-737 positively altered the colonic mucosa and ameliorated inflammation, as shown by colonoscopy, histology and colon length. A decreased BIM/BCL-2 ratio or absence of BIM in both Bim(-/-) and Il10(-) (/) (-) × Bim(-/-) impeded the protective effect of ABT-737. The BIM/BCL-2 ratio decreased with age and during the course of treatment. Thus, long-term treatment resulted in adapted TNF levels and macroscopic mucosal damage. ABT-737 was efficacious in diminishing lymphocytes and ameliorating colitis in a BIM-dependent manner. Regulation of inappropriate survival of lymphocytes by ABT-737 may provide a therapeutic strategy in IBD.

DOI: https://doi.org/10.1111/cei.12635

Increased lymphocyte apoptosis in mouse models of colitis upon ABT-737 treatment is dependent on BIM expression

Christian Lutz[1#] and Mahdi Mozaffari[1#], Vinko Tosevski [4], Michaela Caj[1], Pietro Cippà[2], Bradford L. McRae[3], Candace L. Graff[3], Gerhard Rogler[1], Michael Fried[1], Martin Hausmann[1]

[1] Division of Gastroenterology and Hepatology, Department of Internal Medicine, University Hospital Zurich, Switzerland
[2] Division of Nephrology, University Hospital Zurich, Switzerland
[3] AbbVie Bioresearch Center, AbbVie Worcester, MA
[4] Flow Cytometry Facility, University Zürich, Switzerland
[#] equal contribution

Address for correspondence:

PD Dr. Martin Hausmann
Clinic of Gastroenterology and Hepatology
Department of Internal Medicine, LAB H14 Mail: martin.hausmann@usz.ch
University Hospital of Zürich Tel.: +41 44 255 9916
CH-8091 Zürich Fax.: +41 44 255 9496

Key words: Apoptosis, ABT-737, BIM, BCL-2, IBD, mucosal T cell turnover

Running head Apoptosis by ABT-737 in colitis is BIM dependent

Disclosure: CL, MM, VT, MC, PC, MF and MH have no conflicts of interest to disclose. GR discloses grant support from AbbVie, Ardeypharm, MSD, FALK, Flamentera, Novartis, Roche, Tillots, UCB and Zeller. BLM and CLG are employees of AbbVie, BLM and CLG provided ABT-737, performed MS analysis and further contributed to the discussion of the data, however, AbbVie did not provide any additional financial support (e.g., writing/editing of the manuscript).

Financial support: This research was supported by grant IBD-0324R from the Broad Medical Research Foundation (BMRF) to MH. This research was also supported by grant Project N°2013-16 from the Swiss inflammatory bowel disease cohort study (SIBDCS) to MH and by grant Project 314730_152895 / 1 from the Swiss National Science Foundation.

List of how each author was involved with the manuscript:

- study concept; Hausmann
- acquisition of data; Lutz, Mozaffari, Tosevski, Caj, McRae, Graff, Hausmann
- critical revision of the manuscript; Lutz, Cippa, McRae, Graff, Fried, Rogler

Abbreviations: Azathioprine (AZA), Inflammatory bowel disease (IBD), intestinal epithelial cells (IECs), ulcerative colitis (UC), Crohn's disease (CD)

Abstract

Introduction: Exaggerated activation of lymphocytes contributes to the pathogenesis of inflammatory bowel disease (IBD). Medical therapies are linked to the BCL-2 family-mediated apoptosis. Imbalance in BCL-2 family proteins may cause failure in therapeutic responses. We investigated the role of BCL-2 inhibitor ABT-737 for lymphocyte apoptosis in mice under inflammatory conditions.

Methods: B.6129P2-Il10^{tm1Cgn}/J (*IL-10*$^{-/-}$) weighing 25-30 g with ongoing colitis were used. 50 mg/kg/day ABT-737 was injected i.p. Hematological analyses were performed with an ADVIA 2120 flow cytometer and mass cytometry with a CyTOF 2.

Results: Following i.p. administration ABT-737 was detected in both spontaneous and acute colitis in peripheral blood (PBL) and colon tissue. Treatment lead to lymphopenia. CD4$^+$ CD44$^+$ CD62L$^+$ central memory and CD8$^+$, CD44$^+$ CD62L$^-$ central memory T cells were decreased in PBL upon ABT-737 compared to vehicle-receiving controls. Increased apoptosis upon ABT-737 was determined in blood lymphocytes, splenocytes and Peyer's patches and was accompanied by a decrease in *TNF* and *IL-1B*. ABT-737 positively altered the colonic mucosa and ameliorated inflammation as shown by colonoscopy, histology and colon length. A decreased *BIM* / *BCL-2* ratio or absence of BIM in both *Bim*$^{-/-}$ and *Il10*$^{-/-}$ x *Bim*$^{-/-}$ impeded the protective effect of ABT-737. *BIM* / *BCL-2* ratio was decreased with age and over the course of treatment. Thus long-term treatment resulted in adapted *TNF* levels and macroscopic mucosal damage.

Discussion: ABT-737 was efficacious in diminishing lymphocytes and ameliorating colitis in a BIM dependent manner. To regulate inappropriate survival of lymphocytes by ABT-737 may provide a therapeutic strategy in IBD.

INTRODUCTION

The BCL-2 family plays a critical role in controlling immune responses by regulating the expansion and contraction of the activated lymphocyte population via apoptosis. The majority of activated T cells die at the end of a T cell response, which coincides with the exhibition of decreased levels of BCL-2 just before they begin to die *in vivo* (1). A decrease of the pro-survival BCL-2 contributes to apoptosis of activated T cells (2). In patients suffering from IBD, the lifespan of antigen-primed and activated T cells is extended and an abnormal population of activated T cells is retained within the mucosal compartment (3-5). Enhanced expression of anti-apoptotic BCL-2 is found in lamina propria lymphocytes from inflamed CD tissue after CD2 pathway stimulation (3). Elevated BCL-2 level is also found in cultures of unstimulated T cells isolated from inflamed CD tissue (3). Lamina propria T cells in CD show an activation of the STAT-3 signalling pathway in response to IL-6. STAT-3 mediates the expression of anti-apoptotic genes such as *BCL-2* and *BCL*-XL (6). Resistance of CD T cells to apoptotic signals is correlated with an increased BCL-2 expression (3). This is further supported by reports of a higher BCL-2/BAX ratio in CD mucosa compared to controls (4) as well as a resistance to Fas-induced apoptosis in peripheral T cells acquired from CD patients (7). Apoptosis of anti-inflammatory regulatory T cells (Treg cells) is reduced in both mucosal and peripheral $CD4^{+}CD25^{high}Foxp3^{+}$ Treg cells of IBD patients (8).

Anti-apoptotic BCL-2 interacts with the pro-apoptotic BH3-only protein family member BIM to regulate the survival of lymphocytes. The summary effect of the interaction between BCL-2 and BIM is dependent on the cell type but is also tissue specific, whereby BCL-2 promotes the survival of naïve T cells (9). Indeed, naïve T cells from *Bim*$^{+/-}$ *Bcl-2*$^{-/-}$ mice die at an accelerated rate *in vitro*. BCL-2 is critical in preventing

the pro-apoptotic effects of BIM in naïve $CD8^+$ T cells *in vivo,* but molecules other than BCL-2 may antagonize BIM in $CD4^+$ cells. BIM controls T cell numbers in the periphery by promoting apoptosis and/or decreasing their thymic production. *Bim*-deficient mice have elevated numbers of normal single positive T cells in the periphery (10). Furthermore, BIM is a primary trigger for killing B-cells during their development (11). *Bim* deficiency prevents the death of activated T cells *in vitro* and *in vivo*, suggesting that the protective effect of BCL-2 is mediated solely by neutralization of BIM (2).

Inflammatory bowel disease (IBD) affects about one in a hundred and fifty people in the industrialized world. IBD is characterized by a chronic inflammation of the intestinal wall and comprises two main conditions, namely ulcerative colitis (UC) and Crohn's disease (CD). In the pathogenesis of IBD this inflammatory state is sustained by an exaggerated response of T-lymphocytes to luminal antigens associated with an increased resistance to the induction of apoptosis (4).

Central elements of medical therapy consist of sulfasalazine, aminosalicylates, steroids, immunomodulators and biologicals (12, 13). Medical therapies that regulate lymphocyte proliferation and contraction are directly linked to the BCL-2 family-mediated apoptosis. Sulfasalazine is a potent pro-apoptotic agent (14) as confirmed in peripheral blood lymphocytes from CD patients and in lamina propria T-lymphocytes isolated from inflammatory lesions in CD patients. Induction of apoptosis by sulfasalazine is associated with a decrease in anti-apoptotic BCL-XL and BCL-2. Glucocorticoids inhibit the synthesis of IL-1 and IL-2, resulting in the suppression of the T cell-dependent immune reaction and T cell proliferation (15). Azathioprine (AZA) is an immunosuppressive agent which interferes with T cell-proliferation via its metabolite 6-thioguaninnucleotide. AZA therapy reduces natural killer cells in blood and lamina propria by increasing apoptosis (16). Increased early

and late apoptosis upon AZA was determined in $CD4^+$ T cells from peripheral blood isolated from control patients but not from CD patients (17). BCL-XL is suppressed by AZA, therefore leading to apoptosis through a mitochondrial pathway (18). Anti-TNF antibodies are used in CD and UC to induce and maintain remission. Infliximab was shown to induce apoptosis and an increase in the Bax/Bcl-2 ratio of CD3/CD28 stimulated Jurkat T cells (19). Furthermore the activation of BAX and BAK triggers apoptosis in lamina propria lymphocytes and monocytes by activating the caspase family and inducing cytochrome c release (20). Administration of all clinically effective anti-TNF antibodies resulted in a significant induction of T cell apoptosis in IBD when lamina propria $CD4^+$ T cells expressing $TNFR2^+$ were co-cultured with $mTNF^+$ $CD14^+$ intestinal macrophages (21).

Boosting the initiation of cell death in apoptosis-resistant lymphocytes could improve the success of medical therapy. ABT-737 (AbbVie) is a potent inhibitor of BCL-2, BCL-XL, BCL-W (22, 23) and has been shown to disrupt the interactions of BCL-2 family proteins to induce apoptosis in cancer. ABT-737 inhibits BCL-2 by directly blocking BIM-binding sites and displacing BIM, which becomes freely available to interact with other BCL-2 molecules in the cell. Additionally BIM can bind to BAX and BAK to trigger apoptosis by initiating the formation of pores on the mitochondrial surface. ABT-737 is a BH3-only mimetic that shows a potent action against various transformed cells while exhibiting minimal toxicity toward normal cells. ABT-737 is effective in treating animal models of autoimmune diseases (24), arthritis (25) and lupus (26). Furthermore, expression of BIM, and the extent of its association with BCL-2, correlates with *in vivo* ABT-737 sensitivity (27).

Own studies on apoptosis of lymphocytes in the intestinal mucosa revealed that cell death in Peyer's patches is dependent on the pro-apoptotic protein BIM (28). Based

on these findings we investigated the role of ABT-737 in the cell death of lymphocytes in mice under inflammatory conditions.

MATERIALS AND METHODS

Ethical Considerations

The experimental protocol was approved by the local Animal Care Committee of the University of Zurich (Cantonal Ethics Committee of Zurich, 162/2011).

ABT-737 treatment

ABT-737 was provided by AbbVie Bioresearch (USA) and was injected intra-peritoneally (i.p.) at a dose of 50 mg/kg/day. The vehicle consisted of polyethylene glycol, Tween 80, dextrose solution and DMSO.

Murine colitis models

Acute dextran sulfate sodium (DSS)-induced colitis: B6.129-Bcl2l11tm1.1Ast/J (*Bim*$^{-/-}$) mice were kindly provided by Professor Dr Andreas Villunger (Division for Developmental Immunology, Innsbruck Medical University). *Bim*$^{-/-}$ mice were back-crossed for at least 12 generations. Acute colitis was induced in female C57-BL/6J-Fue and *Bim*$^{-/-}$ mice by administration of 2 % DSS over nine days. Mice weighing 20-25 g were used for the experiments and housed in individually ventilated cages (IVC). All animals were housed for at least three weeks prior to testing in a specific pathogen free (SPF) facility. Animals were sacrificed on day nine. Acute DSS-induced colitis is an animal model for acute intestinal barrier disturbance and acute damage.

Spontaneous colitis: B.6129P2-Il10^{tm1Cgn}/J (*Il10*$^{-/-}$, mice were ordered from The Jackson Laboratory and were already backcrossed to the C57BL/6J genetic background for several generations) and B.6129P2-Il10^{tm1Cgn}/J x B6.129-Bcl2l11$^{tm1.1Ast}$/J (*Il10*$^{-/-}$ x *Bim*$^{-/-}$) develop colitis after 12-15 weeks under SPF

conditions. Il10$^{-/-}$ weighing 25-30 g were used for the experiments. Animals were sacrificed on day 14 of ABT-737 treatment. The Il10$^{-/-}$ model of colitis reflects the exaggerated immune reaction against the endogenous gut flora as seen in CD patients. *Il10*$^{-/-}$ have a low penetrance of disease when raised under SPF conditions, and therapeutic studies in this model are difficult to perform. Therefore we defined a clearly visible rectal prolapse as external visible indicator of ongoing colitis in our *Il10*$^{-/-}$ colony as also stated in the results section whenever *Il10*$^{-/-}$ suffering from ongoing colitis were used.

Assessment of colonoscopy and histological score in mice

Animals were anesthetized with isoflurane and examined with the Tele Pack Pal 20043020 (Karl Storz Endoskope, Germany) and scored according to the murine endoscopic index of colitis severity (MEICS) as previously described (29). For the assessment of the histological scores, 1 cm of the distal third of the colon was removed and scored as described (30, 31).

Cell isolation

Murine peripheral blood lymphocytes were used for mass cytometric analyses. Whole blood was collected in EDTA-treated collection tubes (BD vacutainer, REF 367525). ACK (1,5M NH4Cl, 100mM KHCO3, 10mM Triplex111, ph 7.2) lysing buffer was used for lysing red blood cells.

Splenocytes were isolated using the gentleMACS octo dissociator (Miltenyi, #130-095-937) and gentleMACS C tubes (Miltenyi, #130-093-237). One mouse spleen was transferred into a gentleMACS C tube containing 10ml ACK. A single-cell suspension was obtained by using the gentleMACS octo dissociator program m_spleen 03 for three times. Splenocytes were passed over a 70 µm mesh filter and centrifuged.

Cells were resuspended in 1ml ACK, centrifuged, resuspended in PBS and passed over a 70 µm mesh filter again to obtain 200 – 300 x 10^6 splenocytes/spleen.

Lamina propria mononuclear cells (LPMNC) from small bowel were isolated with the help of the *lamina propria* dissociation kit (Miltenyi, #130-097-410) according to the manufacturer's protocol.

Mass cytometry, staining, data acquisition and analysis

Single cell suspensions obtained from peripheral blood, spleen and lamina propria were stained according to the manufacturer's recommendations (MaxPar Cell Surface Staining Protocol and MaxPar Cytoplasmic/Secreted Antigen Staining Protocol). In short, for viability staining cells were washed with PBS and resuspended in PBS to a maximum concentration of 1x10^7/mL. Cell-ID Cisplatin reagent (Fluidigm, cat. no. 201064) was added to a final concentration of 5 µM. Following 5 minutes incubation at room temperature, samples were washed with cell staining buffer (Fluidigm, cat. no. 201068) by adding 5X the volume of the initial cell suspension. Each sample was resuspended in a volume of 50 µL of cell staining buffer and 50 µL of the surface antibody cocktail was added (MaxPar Mouse Spleen/Lymph Node Phenotyping Panel Kit, cat. no. 201306). Following 30 minutes incubation at room temperature, samples were washed twice with 2mL of cell staining buffer each and fixed by adding 1 mL of 1X MaxPar Fix I Buffer (Fluidigm, cat. no. 201065) to each tube, gently vortexed and incubated at room temperature for additional 15 minutes. Cells were washed twice with 2 mL of MaxPar Perm-S buffer each (Fluidigm, cat. no. 201066) and resuspended in 50 µL of the same buffer. The intracellular antibody cocktail (MaxPar Mouse Intracellular Cytokine I Panel Kit, cat. no. 201310) was added to each sample in 50uL volume and incubated for 30 minutes at room temperature. Following two washing steps with 2 mL of cell staining buffer each, cells

were labeled with 1 mL of 100 nM iridium intercalation solution (Fluidigm, cat. no. 201192B) in MaxPar Fix and Perm buffer (Fluidigm, cat. no. 201067) at 4 °C overnight. Cells were washed twice with 2 mL cell staining buffer each and once with water (Merck Milipore Ultrapure Mili-Q water, 18.2 MΩ*cm@25°C). Cells were left pelleted until ready for acquisition, at which point their concentration was adjusted to 1-1.5 x 10^6 cells/mL in the Ultrapure Mili-Q water.

Cells were acquired on the CyTOF 2 instrument (Fluidigm, USA) with an acquisition flow rate of 0.045mL/min and following data processing settings (default thresholding scheme, lower convolution threshold of 200 IU, minimum event duration of 12 pushes, maximum event duration of 100 pushes, noise reduction active). All samples were spiked with EQ four element calibration beads during acquisition (Fluidigm, cat. no. 201078) and resulting FCS files were normalized according to the built-in normalization algorithm (CyTOF software version 6.0.626) to account for intra- and inter-sample intensity measurement variability. Resulting data was analyzed with FlowJo (Flowjo LLC, USA) and Cytobank (Cytobank Inc, USA) software.

Blood analyses

Hematological analyses were performed by the Division of Hematology at the University Hospital Zurich with an ADVIA 2120 flow cytometer (Siemens, Eschborn, Germany).

RNA extraction and quantitative real time PCR

Total RNA was extracted using the RNeasy Mini Kit (Qiagen, Switzerland). mRNA was reverse transcribed into cDNA using High Capacity cDNA Reverse Transcription Kit (Applied Biosystems, USA). *Bim* (#Mm00437796_m1, Applied Biosystems)*, Bcl-2* (#Mm00477631_m1*), *TNF* (#Mm99999068_m1) and *IL1b* (#Mm01336189_m1)

gene expression was determined with a TaqMan® Gene Expression Assay. Actin gene expression was measured as endogenous control (#4352341E; Applied Biosystems) and used for the calculation of relative mRNA expression by the ΔΔCt method. All samples were analyzed as triplicates.

Analysis of apoptosis and flow cytometry

Apoptosis was quantified by Terminal deoxynucleotidyl transferase dUTP nick end labelling (TUNEL) technology with the In Situ Cell Death Detection Kit (#11684795910, Roche, Mannheim, Germany) as described by the manufacturer.

Numbers of living and apoptotic cells were determined by flow cytometry of annexin V- and PI-stained cells. Cells were resuspended in annexin V binding buffer as indicated by the manufacturer and stained with APC-conjugated annexin V (Enzo Life Science, Switzerland; diluted 1:40) and propidium iodide (PI; Sigma-Aldrich; final concentration 25 µg/ml). Annexin V^- / PI^- cells were considered alive, apoptotic cells displayed staining for annexin V but not for PI.

Fluorescence was measured by flow cytometry using a BD FACSCanto II flow cytometer equipped with two lasers (excitation wave lengths: 488 nm and 633 nm). CD4 was stained with anti-mouse antibody from ImmunoTools (#22150043sp, 1:1000). CD8 was stained with anti-mouse antibody from ImmunoTools (#22150083sp, 1:1000). Both primary antibodies were directly conjugated with FITC.

Statistical analyses

Real time PCR data were calculated from triplicates. Statistical analyses were performed using PASW statistics 18.0 (SPSS Inc., USA). Kruskal-Wallis non-parametric analysis of variance and Bonferroni-corrected Mann-Whitney rank sum test were applied for animal experiments. Box plots express median with relative

quartiles, minimum and maximum. One-Way ANOVA and Tukey Post Hoc test were used for cell culture experiments. Bars represent mean values with whiskers displaying standard deviation. Differences were considered significant at $p < 0.05$ (*), highly significant at $p < 0.01$ (**) and very highly significant at $p < 0.001$ (***).

RESULTS

ABT-737 is detected in blood and intestine following i.p. administration

ABT-737 was applied in the *Il10*$^{-/-}$ model of spontaneous colitis. A calculated dose of 50mg/kg/day was injected i.p. for 14 days. Control mice received a corresponding dose of vehicle solution over the same time-period. No treatment-related death or evidence of infection was observed in any of the animals. Water consumption was not reduced in mice treated with ABT-737 compared to controls. Peripheral blood, feces, intestinal epithelial cells (IEC) and whole colon tissue of mice were harvested (n = 4 each). By mass spectrometric (MS) quantification ABT-737 could be detected in the peripheral blood. Following 14 days of treatment, ABT-737 was localized in peripheral blood (0.47 ± 0.26 µg/µL), feces (9.44 ± 4.12 µg/g), IECs (6.07 ± 6.20 µg/g) and whole colon tissue (3.67 ± 3.91 µg/g). This confirms that following i.p. administration ABT-737 indeed reaches the peripheral blood. MS quantification proved the presence of ABT-737 in whole colon tissue, its uptake into IEC and its accumulation in the feces.

Additionally ABT-737 was applied in the murine model of acute DSS-induced colitis. 50mg/kg/day was injected i.p. for nine days. By MS quantification ABT-737 could be detected in the peripheral blood (0.74 ± 0.37 µg/µL), feces (29.96 ± 21.17 µg/g), IECs (1.61 ± 2.90 µg/g) and whole colon tissue (7.17 ± 0.93 µg/g).

ABT-737 induces a significant lymphopenia in mouse models of colitis

Flow cytometry was performed to quantify viability of lymphocytes upon absorbed ABT-737 in *Il10*$^{-/-}$ mice. The relative number of live PBL was significantly reduced in *Il10*$^{-/-}$ upon ABT-737 compared to controls (45.4 ± 17.4 %, n = 8 vs. 82.4 ± 4.8 %, n = 8 respectively, $p < 0.05$, figure 1 A). Hematological analyses were performed in

the *Il10*$^{-/-}$ model of spontaneous colitis to determine whether the significant increase in number of apoptotic cells upon ABT-737 was associated with a shift in cell populations. The lymphocyte fraction was significantly reduced in *Il10*$^{-/-}$ mice after 14 daily injections of ABT-737 when compared to vehicle-receiving controls (45.9 ± 16.1 %, n = 8 vs. 67.2 ± 14.0 %, n = 8 respectively, $p < 0.05$, figure 1 B). The absolute number of lymphocytes was significantly reduced in *Il10*$^{-/-}$ upon ABT-737 compared to controls (0.53 ± 0.37 x 10^3 cells/µL, n = 8 vs. 1.83 ± 0.83 x 10^3 cells/µL, n = 8 respectively, $p < 0.05$). In accordance the combined granulocyte and monocyte-fraction was significantly increased in ABT-737-treated *Il10*$^{-/-}$ mice (49.3 ± 14.8 %, n = 8 vs. 24.6 ± 11.1 %, n = 8 respectively, $p < 0.05$, figure 1 C). The absolute number of the combined granulocyte and monocyte-fraction was reduced in *Il10*$^{-/-}$ upon ABT-737 compared to controls (0.54 ± 0.18 x 10^3 cells/µL, n = 8 vs. 0.88 ± 0.48 x 10^3 cells/µL, n = 8 respectively) however not significantly different. In contrast erythrocyte counts were not affected (9.13 ± 0.83 x 10^{12} cells/L, n = 8 vs. 8.96 ± 0. 87 x 10^{12} cells/µL, n = 8). As inhibition of BCL-2 by ABT-737 is mediated by displacing the pro-apoptotic factor BIM we also applied ABT-737 in *Il10*$^{-/-}$ x *Bim*$^{-/-}$. Both the fraction of lymphocytes (78.8 ± 10.1 %, n = 5 vs. 81.2 ± 7.5 %, n = 4 respectively, figure 1 B) and of granulocytes and monocytes (10.9 ± 7.8 %, n = 5 vs. 12.8 ± 4.3 %, n = 4 respectively, figure 1 C) were unaltered upon ABT-737. The absolute number of lymphocytes remained unchanged in *Il10*$^{-/-}$ x *Bim*$^{-/-}$ upon ABT-737 compared to controls (6.16 ± 3.61 x 10^3 cells/µL, n = 5 vs. 5.47 ± 3.81 x 10^3 cells/µL, n = 5 respectively) as well as the absolute number of the combined granulocyte and monocyte-fraction (0.90 ± 1.22 x 10^3 cells/µL, n = 5 vs. 1.08 ± 0.71 x 10^3 cells/µL, n = 5 respectively). PBL from colitic *Il10*$^{-/-}$ mice were analyzed by mass cytometry. TCRβ$^+$, CD3$^+$, CD4$^+$ were analyzed for CD44 and CD62L expression (figure 1 D). The proportion of CD44$^+$ CD62L$^+$ central memory T cells was decreased upon ABT-

737 (10.4 ± 7.4 %, n = 3) compared to vehicle-receiving controls (23.8 ± 8.1, n = 3). The proportion of TCRβ$^+$, CD3$^+$, CD8$^+$, CD44$^+$ CD62L$^-$ central memory T cells was decreased upon ABT-737 (17.9 ± 11.5 %, n = 3) compared to vehicle-receiving controls (34.2 ± 24.0, n = 3).

Additionally hematological analyses for C57-BL/6J-Fue mice with a DSS-induced acute colitis confirmed significantly reduced absolute lymphocyte count upon ABT-737 compared to controls (supplemental figure 1 A). ABT-737 levels in peripheral blood determined by MS were directly correlated to the removal of lymphocytes, as well as an increased relative number of granulocytes and monocytes (supplemental figure 1 C). The absolute number of the combined granulocyte and monocyte-fraction was reduced in mice suffering from DSS-induced colitis upon ABT-737 compared to controls (1.04 ± 0.68 x 10^3 cells/µL, n = 12 vs. 1.42 ± 1.04 x 10^3 cells/µL, n = 12 respectively) however not significantly different. In flow cytometry CD8$^+$ appeared to be diminished upon ABT-737 treatment, although the differences were not significant (7.8 ± 3.2 %, n = 10 vs. 10.7 ± 6.2 %, n = 12 respectively).

The decrease in lymphocyte counts is accompanied by a reduction of pro-inflammatory cytokines

We determined whether the significant decrease of lymphocyte counts in *Il10*$^{-/-}$ mice was associated with a decrease in *TNF* and *IL1b* gene expression upon ABT-737 treatment. The cytokine profile of *Il10*$^{-/-}$ mice was assessed in peripheral blood drawn from the tail vein on days 7 and 14. *TNF* gene expression was significantly decreased on day 14 in ABT-737-treated mice compared to vehicle-treated mice (82 ± 28, n = 8 vs. 241 ± 15, n = 8 respectively, figure 2 A). *IL1b* gene expression was also significantly decreased on day 14 in ABT-737-treated mice (49 ± 27, n = 8

vs. 276 ± 135, n = 8 respectively, figure 2 B). With regards to *Il6* and *Ifng* mRNA expression, no significant changes were recorded.

BIM is required for the protective effect of ABT-737

Splenocytes from colitis *Il10*$^{-/-}$ mice were analyzed by flow cytometry after 14 daily injections of ABT-737. ABT-737 treatment was followed by a significant decrease in CD8^{+} splenocytes in *Il10*$^{-/-}$ mice compared to vehicle-receiving *Il10*$^{-/-}$ mice (15.9 ± 3.3 %, n = 9 vs. 9.2 ± 2.5 %, n = 9 respectively, $p < 0.05$, figure 3 A and B). To elucidate ABT-737-dependent changes in apoptosis in the absence of BIM *Bim*$^{-/-}$ x *Il10*$^{-/-}$ mice were used. In contrast to the results obtained from *Il10*$^{-/-}$ mice there was no detectable difference in CD8^{+} splenocytes from *Bim*$^{-/-}$ x *Il10*$^{-/-}$ mice upon ABT-737 (figure 3 A). This significant decrease in CD3^{+} CD8^{+} splenocytes in *Il10*$^{-/-}$ mice upon ABT-737 compared to vehicle-receiving *Il10*$^{-/-}$ mice (17.5 ± 1.1 %, n = 3 vs. 11.5 ± 1.9 %, n = 3 respectively, $p < 0.05$, statistical analysis was performed using the Holm-Sidak method, figure 3 C) was also confirmed by mass cytometry.

Apoptosis of splenocytes is significantly increased upon ABT-737 treatment

Increased apoptosis in peripheral blood was associated with a reduction of lymphocyte counts in ABT-737-treated mice. The level of cleavage of genomic DNA in spleen in the DSS-induced acute colitis model was analyzed. TUNEL assays revealed an increased apoptosis in mice treated for nine days with ABT-737 (supplemental figure 2 A and B). Apoptosis-positive cells were detectable in the red pulp and to a lesser extent in the white pulp.

Furthermore, ABT-737 treatment was followed by a significant reduction in spleen weight in C57-BL/6J-Fue mice suffering from DSS-induced acute colitis (0.10 ± 0.03 g for vehicle-receiving mice as compared to 0.07 ± 0.02 g for ABT-737-receiving

mice, supplemental figure 2 C and D). This difference in spleen weight was not seen in colitic *Bim*$^{-/-}$ mice upon ABT-737 treatment. Irrespective of the treatment, spleen weight in *Bim*$^{-/-}$ was increased compared to C57-BL/6J-Fue mice, as previously described (supplemental figure 2 C).

ABT-737 significantly increases apoptosis in Peyer's patches

The increased number of TUNEL^{+} cells in the peripheral blood and spleen indicated that the number of lymphocytes was reduced in ABT-737-treated mice. Additionally significantly increased cleavage of genomic DNA was found in Peyer's patches in the *Il10*$^{-/-}$ model in both groups treated for five (supplemental figure 3 A) and 14 days (figure 4 A and B) with ABT-737. Next we isolated LPMNC from small bowel from *Il10*$^{-/-}$ treated for 14 days. Viable cells were identified by cisplatin staining followed by mass cytometry. A certain number of dead cells is certainly due to the isolation procedure, however, significantly increased number of dead cells was found in LPMNC isolated from small bowel in the *Il10*$^{-/-}$ model with ABT-737 compared to vehicle-treated mice (72.9 ± 3.1 %, n = 3 vs. 46.8 ± 12.2 %, n = 3 respectively, $p < 0.05$, Holm-Sidak method, figure 4 C). A decrease in viable CD3^{+} CD4^{+} LPMNC in *Il10*$^{-/-}$ mice upon ABT-737 compared to vehicle-receiving *Il10*$^{-/-}$ mice (4.9 ± 3.8 %, n = 3 vs. 13.3 ± 6.4 %, n = 3 respectively, $p < 0.05$, figure 4 D) was confirmed by mass cytometry. Additionally a decrease in viable CD3^{+} CD8^{+} LPMNC upon ABT-737 (3.6 ± 2.7 %, n = 3 vs. 11.2 ± 6.4 %, n = 3 respectively, $p < 0.05$, figure 4 D) was found.

Although mice suffering from acute DSS-induced colitis do not develop ileitis TUNEL staining also revealed increased apoptosis in Peyer's patches from mice treated for nine days with ABT-737 upon water (supplemental figure 4) or DSS (supplemental figure 5). TUNEL also revealed an increased apoptosis in the *lamina propria* of mice

treated for nine days with ABT-737 (supplemental figure 4 and 5). TUNEL$^+$ cells appeared more frequently as clusters of more than four cells (supplemental figure 6).

ABT-737 ameliorates spontaneous and acute colitis

To determine the influence of ABT-737-dependent on mucosal inflammation and apoptosis both the *Il10*$^{-/-}$ model and the DSS-induced model were used. Macroscopic mucosal damage was assessed by mini-endoscopy. *Il10*$^{-/-}$ mice with a clearly visible rectal prolapse received 50mg/kg/day (n = 18) or vehicle (n = 14) over 14 days. Mice were sacrificed on day 14. *Il10*$^{-/-}$ mice receiving vehicle displayed an opaque mucosa and altered vascular pattern on day 14 (MEICS 6.9 ± 2.3, n = 14, figure 5 A). The thickening of the colon became more prominent, thin feces were discovered and the diseased regions frequently presented with mucosal bleeding. During treatment with ABT-737 inflammation was ameliorated. Compared to vehicle-receiving mice, *Il10*$^{-/-}$ mice treated with ABT-737 had a transparent mucosa with a regular vascular pattern. Solid feces were visible (MEICS 3.6 ± 1.7, n = 18, figure 5 B). No differences in MEICS were determined in *Il10*$^{-/-}$ x *Bim*$^{-/-}$ upon ABT-737 (figure 5 A and B).

Additionally mice upon acute colitis receiving vehicle displayed an opaque mucosa and altered vascular pattern on day 9 (MEICS 4.3 ± 1.8, n = 14, supplemental figure 7). Colon became thickened, extensive amounts of feces were discovered and the diseased regions frequently presented with mucosal bleeding. During treatment with ABT-737 signs of an ameliorated inflammation were found. Mice suffering from DSS-induced acute colitis but treated with ABT-737 had a transparent mucosa with a regular vascular pattern. Solid feces were visible (MEICS 1.4 ± 0.9, n = 13, supplemental figure 7). In contrast, no difference in MEICS was determined in *Bim*$^{-/-}$ mice treated with ABT-737 (supplemental figure 7). In summary ABT-737 positively

altered the colonic mucosa at a macroscopic level in both the *Il10*$^{-/-}$ model of spontaneous colitis and DSS-induced acute colitis.

Colon length was determined in both spontaneous colitis and DSS-induced acute colitis models. In *Il10*$^{-/-}$ mice ABT-737 treatment prevented the shortening in colon length significantly (8.18 ± 0.27 cm vs. 7.65 ± 0.38 cm, respectively, figure 6 A). The histological score of *Il10*$^{-/-}$ mice treated with ABT-737 was significantly lower as in untreated mice (figure 6 B). ABT-737-treated *Il10*$^{-/-}$ mice had less lymphocyte influx in the thickened lamina propria (figure 6 C). Compared to vehicle-receiving mice, *Il10*$^{-/-}$ mice treated with ABT-737 showed increased body weight (figure 6 D) however not significantly different.

In C57-BL/6J-Fue mice, induction of DSS-induced acute colitis was followed by a significant reduction in colon length (supplemental figure 8 A). ABT-737 treatment prevented the shortening in colon length significantly in DSS-induced colitis (7.44 ± 0.51 cm, n = 18 vs. 6.35 ± 0.57 cm, n = 18, $p < 0.001$, respectively, supplemental figure 8 A). The number of lymphocytes in colonic mucosa was determined and immunohistochemistry applying anti-CD3 antibody was performed. $CD3^+$ cells in the acquired images were appropriately marked and quantified by an investigator blinded to the experiment setup. Immunohistochemistry revealed a decreased number of $CD3^+$ in the colonic *lamina propria* of mice treated for nine days with ABT- (49.5 ± 39.5 cells/hpf, n = 16 hpfs and 70.1 ± 30.4 cells/hpf, n = 14 hpfs, respectively, supplemental figure 8 B).

$CD4^+CD62L^+$ are susceptible for priming with ABT-737 but *Bcl-2* increases during ongoing inflammation

We assessed ABT-737-dependent priming for apoptosis in lymphocyte sub-populations. *Il10*$^{-/-}$ with a clearly visible rectal prolapse received either a dose of 50mg/kg/day ABT-737 (n = 5) or vehicle (n = 5) for 14 days as *in vivo* pre-treatment. $CD4^+CD62L^+$ were isolated from the splenocytes and incubated for 12h with ABT-737 or vehicle. Following ABT-737 *in vivo* pre-treatment $CD4^+CD62L^+$ cells became significantly more susceptible to apoptosis initiated by ABT-737 compared to vehicle controls (figure 7 A). According contour plots for are shown in supplemental figure 9. Furthermore, *BIM* and *BCL-2* gene expression in $CD4^+CD62L^+$ and $CD4^+CD62L^-$ cells after pre-treatment with either ABT-737 or vehicle was determined. The *BIM* / *BCL-2* ratio was significantly decreased on day 14 in $CD4^+CD62L^+$ from ABT-737-treated mice compared to vehicle treated mice (26 ± 8, n = 5 vs. 87 ± 13, n = 5 respectively, figure 7 B). *In vivo* pre-treatment with ABT-737 lowered the *BIM* / *BCL-2* ratio in $CD4^+CD62L^+$. As the *BIM* / *BCL-2* ratio was significantly decreased on day 14 in $CD4^+CD62L^+$ from ABT-737-treated mice *BCL-2* and *BCL-XL* gene expression in $CD4^+CD62L^+$ cells in relation to age and treatment was determined. $CD4^+CD62L^+$ from Il10$^{-/-}$ 8 weeks of age (n = 5) were compared to 12 weeks old mice with (n = 5) and without ABT-737 treatment (n = 5). 8 week-old mice without visible rectal prolapse were compared with 12 week-old mice with either a visible or a developing rectal prolapse. *BCL-2* gene expression was significantly increased in older mice compared to younger mice. *BCL-2* was also significantly increased upon ABT-737 compared to vehicle control (figure 7 C).

Apoptosis stimulating effect is decreased upon ABT-737 long-term treatment

Long term treatment with ABT-737 in *Il10*$^{-/-}$ mice was performed. *Il10*$^{-/-}$, at 8 weeks of age, with no signs of rectal prolapse, received either 50mg/kg ABT-737 every three days (n = 10) or vehicle (n = 10) over a period of 56 days. Treatment was applied i.p. Long term treatment with ABT-737-induced depigmentation of the abdominal skin, whereas the head, chest and back were not affected (supplemental figure 10).

Il10$^{-/-}$ were sacrificed on day 56. 7 mice upon ABT-737 and 8 vehicle-treated mice developed a clearly visible rectal prolapse during the experiment. Macroscopic mucosal damage was assessed by mini-endoscopy and colonoscopy score on day 14 and on day 55. On day 55 *Il10*$^{-/-}$ mice from both groups displayed an opaque mucosa and altered vascular pattern (figure 8 A). The thickening of the colon became more prominent, thin feces were discovered and the diseased regions frequently presented with mucosal bleeding. (MEICS 10.0 ± 2.5, n = 5 for mice devoid of ABT-737 compared to 11.1 ± 2.9, n = 5 for mice upon ABT-737, figure 8 B).

The cytokine profile in peripheral blood was assessed on days 0, 14, 28, 42 and 56 without further pre-stimulation of lymphocytes at mRNA level (figure 8 C). In support of data from short time-frame experiments mentioned above, *TNF* gene expression was significantly decreased on day 14 in ABT-737-treated mice compared to vehicle-treated mice. No significant changes were recorded between treatment with ABT-737 and vehicle on day 56.

DISCUSSION

As dysregulated apoptosis of activated lymphocytes driven by increased anti-apoptotic BCL-2 and BCL-XL contributes to the pathogenesis of IBD (3, 4, 6, 7, 32) we analyzed the potential of the priming agent ABT-737 to limit the persistence of lymphocytes in mouse models of colitis.

In the present study, we applied pro-apoptotic ABT-737 in both the murine model of acute DSS-induced colitis and the *Il10*$^{-/-}$ model of spontaneous colitis. Following i.p. administration ABT-737 was detected in peripheral blood, colon tissue and IEC. We determined ABT-737 accumulation in the feces. ABT-737 treatment lead to lymphopenia in mice demonstrated by the reduced lymphocyte and thrombocyte counts as well as the increased fraction of combined granulocytes and monocytes compared to controls. PBL were cleared in a dose-dependent manner upon ABT-737 and proportions of $CD8^+$ appeared to be diminished. Increased apoptosis upon ABT-737 was determined in PBL, splenocytes and Peyer's patches and was accompanied by a decrease in *TNF* and *IL1b* gene expression compared to vehicle-control. $CD4^+$ $CD44^+$ $CD62L^+$ central memory T cells were decreased in PBL upon ABT-737 compared to vehicle-receiving controls. $CD8^+$, $CD44^+$ $CD62L^-$ central memory T cells were also decreased upon ABT-737. Naïve T cells require both MCL-1 and BCL-2 for survival (Ivan Dzhagalov *et al.*). In our own experiments $CD4^+$ naïve T cells are hardly affected by ABT-737 which is not inhibiting MCL-1. This may protect T cell sub-populations from initiation of apoptosis and contribute to a low *BIM* / *BCL-2* ratio in remaining cells. ABT-737 positively alters the colonic mucosa at both macroscopic and microscopic level, while also ameliorating intestinal inflammation in models of colitis as shown by MEICS, histological score and colon length. Inactivation of BCL-2 is key to the ability of BIM to induce apoptosis. BIM can also directly bind to pro-

apoptotic BAX and BAK in order to initiate apoptosis (33). Other BH3-only proteins such as BMF, BAD, NOXA and PUMA are considered to act as sensitizers which bind the pro-survival BCL-2 protein and thereby displace BIM from BCL-2 to promote cell death (34). As inhibition of BCL-2 by ABT-737 is mediated by BIM we also applied ABT-737 to both *Il10*$^{-/-}$ x *Bim*$^{-/-}$ upon spontaneous colitis and *Bim*$^{-/-}$ upon DSS-induced acute colitis and confirmatively mice were found to be relatively resistant to the lymphocyte apoptosis upon ABT-737 administration. In our own experiments we could also show that following 14 days of ABT-737 pre-treatment *in vivo,* gut-homing $CD4^+CD62L^+$ cells became more susceptible to apoptosis compared to vehicle controls. *BIM* / *BCL-2* balance is critical for maintaining T cell homeostasis (9). However, the *BIM* / *BCL-2* ratio was decreased with age and over the course of treatment in our own experimental setup. Thus long-term treatment over a period of 56 days resulted in adapted *TNF* levels and macroscopic mucosal damage.

ABT-737 affects various transformed cells, while exhibiting minimal toxicity toward normal cells. Navitoclax, the orally administered form of ABT-737, has been applied in chronic lymphocytic leukemia (CLL). CLL is characterized by the accumulation of lymphocytes, typically of B-cell origin, in the blood, lymph nodes and spleen. In a phase I study of 26 patients, nine achieved a partial response and seven maintained stable disease for more than 6 months (35). Furthermore, the expression of Bim, and the extent of its association with Bcl-2, correlates with *in vivo* ABT-737-sensitivity in CLL (27). Navitoclax has also been successfully tested in small cell lung cancer xenograft models. Although Navitoclax exhibited an important range of antitumor activity, leading to complete tumor regression in several models (36), Bcl-2 targeting by navitoclax showed limited single-agent activity against advanced and recurrent small cell lung cancer in a phase II study (37).

Studies observing ABT-737 in inflammatory conditions characterized by the uncontrolled proliferation of lymphocytes yielded results which corroborated our own findings. ABT-737 was efficacious in reducing accumulated lymphocytes associated with tissue and organ damage in other animal models of autoimmunity. Collagen-induced arthritis in DBA/J mice is a well-established rodent model for rheumatoid arthritis, which is clinically characterized by paw swelling leading to ankylosis. Treatment with ABT-737 and dexamethasone significantly reduced the mean arthritic score and paw swelling compared with the vehicle-treated group (24). ABT-737 treatment was associated with lymphocyte and platelet depletion. In parallel ABT-737 was applied in a murine model of delayed-type hypersensitivity (DTH) in C57BL/6 mice. The DTH test is used to determine whether a prior exposure to a specific antigen has occurred. This reaction has been shown to be dependent on CD4+ and CD8+ memory T cells. Treatment with ABT-737 and dexamethasone showed a similar reduction in paw swelling compared to the vehicle-treated group (24). ABT-737 was also applied in a murine model of Ifng-induced lupus nephritis. Treatment with ABT-737 prolonged survival and reduced glomerulonephritis to a similar extent to that observed with mycophenolate mofetil (24). In animal models of systemic lupus erythematosus a decrease in lymphocyte apoptosis is clearly associated with more severe disease pathogenesis. Both Bcl-2-transgenic mice (38) and Bim-deficient mice (39) show evidence of systemic lupus erythematosus-like clinical symptoms caused by prolonged survival of lymphocytes. In patients with lupus, elevated Bcl-2 expression in lymphocytes has been reported (40).

The regulative function of ABT-737 on uncontrolled proliferation of lymphocytes could be also confirmed with a different approach. ABT-737 suppresses allogeneic T- and

B-cell responses after skin transplantation (41). *In vitro*, ABT-737 prevented allogeneic T cell activation, proliferation, and cytotoxicity by inducing apoptosis. The physiological functions of the remaining viable T cells were not impaired. *In vivo*, ABT-737 was highly selective for lymphoid cells and inhibited allogeneic T- and B-cell responses after skin transplantation.

In recent years the importance of expansion and contraction of activated lymphocytes by apoptosis has been extensively discussed. Failure in the apoptotic mechanism of lymphocyte control can lead to the development of autoimmunity. Inducing the apoptosis of lymphocytes may provide the basis for a new therapeutic strategy in CD patients. Furthermore, investigating the imbalance between pro-and anti-apoptotic proteins could help predict clinical relapse upon standard medical therapy. Ultimately, this knowledge could lead to the development of new therapeutic options for the treatment of IBD, by focusing on controlling the abnormally large population of activated cells and thereby restoring a physiological turnover of lymphocytes and homeostasis.

Disclosure

CL, MM, VT, MC, PC, MF and MH have no conflicts of interest to disclose. GR discloses grant support from AbbVie, Ardeypharm, MSD, FALK, Flamentera, Novartis, Roche, Tillots, UCB and Zeller. BLM and CLG are employees of AbbVie, BLM and CLG provided ABT-737, performed MS analysis and further contributed to the discussion of the data, however, AbbVie did not provide any additional financial support (e.g., writing/editing of the manuscript).

Financial support

This research was supported by grant IBD-0324R from the Broad Medical Research Foundation (BMRF) to MH. This research was also supported by grant Project N°2013-16 from the Swiss inflammatory bowel disease cohort study (SIBDCS) to MH and by grant Project 314730_152895 / 1 from the Swiss National Science Foundation.

Acknowledgements

We thank Professor Dr. Thomas Fehr (Division of Nephrology, University Hospital Zurich, Switzerland) for providing ABT-737, murine intestinal tissue and invaluable help with the start-up of the project.

REFERENCES

1. Mitchell T, Kappler J, Marrack P. Bystander virus infection prolongs activated T cell survival. *J Immunol* 1999; **162**(8)**:** 4527-4535.

2. Hildeman DA, Zhu Y, Mitchell TC, Bouillet P, Strasser A, Kappler J*, et al.* Activated T cell death in vivo mediated by proapoptotic bcl-2 family member bim. *Immunity* 2002; **16**(6)**:** 759-767.

3. Boirivant M, Marini M, Di Felice G, Pronio AM, Montesani C, Tersigni R*, et al.* Lamina propria T cells in Crohn's disease and other gastrointestinal inflammation show defective CD2 pathway-induced apoptosis. *Gastroenterology* 1999; **116**(3)**:** 557-565.

4. Ina K, Itoh J, Fukushima K, Kusugami K, Yamaguchi T, Kyokane K*, et al.* Resistance of Crohn's disease T cells to multiple apoptotic signals is associated with a Bcl-2/Bax mucosal imbalance. *J Immunol* 1999; **163**(2)**:** 1081-1090.

5. Itoh J, de La Motte C, Strong SA, Levine AD, Fiocchi C. Decreased Bax expression by mucosal T cells favours resistance to apoptosis in Crohn's disease. *Gut* 2001; **49**(1)**:** 35-41.

6. Atreya R, Mudter J, Finotto S, Mullberg J, Jostock T, Wirtz S*, et al.* Blockade of interleukin 6 trans signaling suppresses T-cell resistance against apoptosis in chronic intestinal inflammation: evidence in crohn disease and experimental colitis in vivo. *Nat Med* 2000; **6**(5)**:** 583-588.

7. Iborra M, Moret I, Buso E, Rausell F, Bastida G, Aguas M*, et al.* Differential Regulation of Oxidative Stress and Apoptosis Related Genes During Active and Inactive Crohn's Disease (CD). *Gastroenterology* 2012; **142**(5, Supplement 1)**:** S-877.

8. Veltkamp C, Anstaett M, Wahl K, Moller S, Gangl S, Bachmann O*, et al.* Apoptosis of regulatory T lymphocytes is increased in chronic inflammatory bowel disease and reversed by anti-TNFalpha treatment. *Gut* 2011; **60**(10)**:** 1345-1353.

9. Wojciechowski S, Tripathi P, Bourdeau T, Acero L, Grimes HL, Katz JD*, et al.* Bim/Bcl-2 balance is critical for maintaining naive and memory T cell homeostasis. *J Exp Med* 2007; **204**(7)**:** 1665-1675.

10. Bouillet P, Metcalf D, Huang DC, Tarlinton DM, Kay TW, Kontgen F*, et al.* Proapoptotic Bcl-2 relative Bim required for certain apoptotic responses, leukocyte homeostasis, and to preclude autoimmunity. *Science* 1999; **286**(5445)**:** 1735-1738.

11. Tischner D, Woess C, Ottina E, Villunger A. Bcl-2-regulated cell death signalling in the prevention of autoimmunity. *Cell Death Dis* 2010; **1:** e48.

12. Dignass A, Lindsay JO, Sturm A, Windsor A, Colombel JF, Allez M*, et al.* Second European evidence-based consensus on the diagnosis and

management of ulcerative colitis part 2: current management. *J Crohns Colitis* 2012; **6**(10)**:** 991-1030.

13. Dignass A, Van Assche G, Lindsay JO, Lemann M, Soderholm J, Colombel JF*, et al.* The second European evidence-based Consensus on the diagnosis and management of Crohn's disease: Current management. *J Crohns Colitis* 2010; **4**(1)**:** 28-62.

14. Doering J, Begue B, Lentze MJ, Rieux-Laucat F, Goulet O, Schmitz J*, et al.* Induction of T lymphocyte apoptosis by sulphasalazine in patients with Crohn's disease. *Gut* 2004; **53**(11)**:** 1632-1638.

15. Bianchi M, Meng C, Ivashkiv LB. Inhibition of IL-2-induced Jak-STAT signaling by glucocorticoids. *Proc Natl Acad Sci U S A* 2000; **97**(17)**:** 9573-9578.

16. Steel AW, Mela CM, Lindsay JO, Gazzard BG, Goodier MR. Increased proportion of CD16(+) NK cells in the colonic lamina propria of inflammatory bowel disease patients, but not after azathioprine treatment. *Aliment Pharmacol Ther* 2011; **33**(1)**:** 115-126.

17. Ben-Horin S, Goldstein I, Fudim E, Picard O, Yerushalmi Z, Barshack I*, et al.* Early preservation of effector functions followed by eventual T cell memory depletion: a model for the delayed onset of the effect of thiopurines. *Gut* 2009; **58**(3)**:** 396-403.

18. Tiede I, Fritz G, Strand S, Poppe D, Dvorsky R, Strand D*, et al.* CD28-dependent Rac1 activation is the molecular target of azathioprine in primary human CD4+ T lymphocytes. *J Clin Invest* 2003; **111**(8)**:** 1133-1145.

19. ten Hove T, van Montfrans C, Peppelenbosch MP, van Deventer SJ. Infliximab treatment induces apoptosis of lamina propria T lymphocytes in Crohn's disease. *Gut* 2002; **50**(2)**:** 206-211.

20. Lugering A, Schmidt M, Lugering N, Pauels HG, Domschke W, Kucharzik T. Infliximab induces apoptosis in monocytes from patients with chronic active Crohn's disease by using a caspase-dependent pathway. *Gastroenterology* 2001; **121**(5)**:** 1145-1157.

21. Atreya R, Zimmer M, Bartsch B, Waldner MJ, Atreya I, Neumann H*, et al.* Antibodies against tumor necrosis factor (TNF) induce T-cell apoptosis in patients with inflammatory bowel diseases via TNF receptor 2 and intestinal CD14(+) macrophages. *Gastroenterology* 2011; **141**(6)**:** 2026-2038.

22. Oltersdorf T, Elmore SW, Shoemaker AR, Armstrong RC, Augeri DJ, Belli BA*, et al.* An inhibitor of Bcl-2 family proteins induces regression of solid tumours. *Nature* 2005; **435**(7042)**:** 677-681.

23. Chen S, Dai Y, Pei XY, Grant S. Bim upregulation by histone deacetylase inhibitors mediates interactions with the Bcl-2 antagonist ABT-737: evidence for distinct roles for Bcl-2, Bcl-xL, and Mcl-1. *Mol Cell Biol* 2009; **29**(23)**:** 6149-6169.

24. Bardwell PD, Gu J, McCarthy D, Wallace C, Bryant S, Goess C*, et al.* The Bcl-2 family antagonist ABT-737 significantly inhibits multiple animal models of autoimmunity. *J Immunol* 2009; **182**(12)**:** 7482-7489.

25. Liu H, Pope RM. The role of apoptosis in rheumatoid arthritis. *Curr Opin Pharmacol* 2003; **3**(3)**:** 317-322.

26. Nagy G, Koncz A, Perl A. T- and B-cell abnormalities in systemic lupus erythematosus. *Crit Rev Immunol* 2005; **25**(2)**:** 123-140.

27. High LM, Szymanska B, Wilczynska-Kalak U, Barber N, O'Brien R, Khaw SL*, et al.* The Bcl-2 homology domain 3 mimetic ABT-737 targets the apoptotic machinery in acute lymphoblastic leukemia resulting in synergistic in vitro and in vivo interactions with established drugs. *Mol Pharmacol* 2010; **77**(3)**:** 483-494.

28. Leucht K, Caj M, Fried M, Rogler G, Hausmann M. Impaired removal of Vbeta8 lymphocytes aggravates colitis in mice deficient for BIM. *Clin Exp Immunol* 2013; **173**(3)**:** 493-501.

29. Becker C, Fantini MC, Wirtz S, Nikolaev A, Kiesslich R, Lehr HA*, et al.* In vivo imaging of colitis and colon cancer development in mice using high resolution chromoendoscopy. *Gut* 2005; **54**(7)**:** 950-954.

30. Obermeier F, Kojouharoff G, Hans W, Scholmerich J, Gross V, Falk W. Interferon-gamma (IFN-gamma)- and tumour necrosis factor (TNF)-induced nitric oxide as toxic effector molecule in chronic dextran sulphate sodium (DSS)-induced colitis in mice. *Clin Exp Immunol* 1999; **116**(2)**:** 238-245.

31. Steidler L, Hans W, Schotte L, Neirynck S, Obermeier F, Falk W*, et al.* Treatment of murine colitis by Lactococcus lactis secreting interleukin-10. *Science* 2000; **289**(5483)**:** 1352-1355.

32. Kruidenier L, Kuiper I, Van Duijn W, Mieremet-Ooms MA, van Hogezand RA, Lamers CB*, et al.* Imbalanced secondary mucosal antioxidant response in inflammatory bowel disease. *J Pathol* 2003; **201:** 17-27.

33. Ewings KE, Wiggins CM, Cook SJ. Bim and the pro-survival Bcl-2 proteins: opposites attract, ERK repels. *Cell Cycle* 2007; **6**(18)**:** 2236-2240.

34. Kutuk O, Letai A. Displacement of Bim by Bmf and Puma rather than increase in Bim level mediates paclitaxel-induced apoptosis in breast cancer cells. *Cell Death Differ* 2010; **17**(10)**:** 1624-1635.

35. Roberts AW, Seymour JF, Brown JR, Wierda WG, Kipps TJ, Khaw SL*, et al.* Substantial susceptibility of chronic lymphocytic leukemia to BCL2 inhibition: results of a phase I study of navitoclax in patients with relapsed or refractory disease. *J Clin Oncol* 2012; **30**(5)**:** 488-496.

36. Shoemaker AR, Mitten MJ, Adickes J, Ackler S, Refici M, Ferguson D*, et al.* Activity of the Bcl-2 family inhibitor ABT-263 in a panel of small cell lung cancer xenograft models. *Clin Cancer Res* 2008; **14**(11)**:** 3268-3277.

37. Rudin CM, Hann CL, Garon EB, Ribeiro de Oliveira M, Bonomi PD, Camidge DR*, et al.* Phase II study of single-agent navitoclax (ABT-263) and biomarker correlates in patients with relapsed small cell lung cancer. *Clin Cancer Res* 2012; **18**(11)**:** 3163-3169.

38. Mandik-Nayak L, Nayak S, Sokol C, Eaton-Bassiri A, Madaio MP, Caton AJ*, et al.* The origin of anti-nuclear antibodies in bcl-2 transgenic mice. *Int Immunol* 2000; **12**(3)**:** 353-364.

39. Hughes P, Bouillet P, Strasser A. Role of Bim and other Bcl-2 family members in autoimmune and degenerative diseases. *Curr Dir Autoimmun* 2006; **9:** 74-94.

40. Miret C, Font J, Molina R, Garcia-Carrasco M, Filella X, Ramos M*, et al.* Bcl-2 oncogene (B cell lymphoma/leukemia-2) levels correlate with systemic lupus erythematosus disease activity. *Anticancer Res* 1999; **19**(4B)**:** 3073-3076.

41. Cippa PE, Kraus AK, Edenhofer I, Segerer S, Chen J, Hausmann M*, et al.* The BH3-mimetic ABT-737 inhibits allogeneic immune responses. *Transpl Int* 2011; **24**(7)**:** 722-732.

Titles and legends to figures

Figure 1 **Cell death upon ABT-737 is selective for PBL**

(A - D) *Il10*$^{-/-}$ and *Il10*$^{-/-}$ x *Bim*$^{-/-}$ mice in the model of spontaneous colitis. (A) Flow cytometry revealed an increased number of PI^{+} cells in PBL upon ABT-737 treatment. Mann-Whitney rank sum test. Treatment with ABT-737 (B) significantly decreased the number of lymphocytes and (C) significantly increased number of granulocytes compared to vehicle. Statistical analysis was performed using ANOVA and All Pairwise Multiple Comparison Procedures (Bonferroni t-test), $p < 0.05$ (*). (D) Mass cytometry revealed a decreased proportion of CD44^{+} CD62L^{+} central memory T cells upon ABT-737 compared to vehicle.

Figure 2: **During spontaneous colitis in *Il10*$^{-/-}$ pro-inflammatory cytokines were significantly decreased upon ABT-737-treatment compared to vehicle-receiving controls.** mRNA expression levels determined by qPCR from (A) *TNF* and (B) *IL1b*. Statistical analysis was performed using the Mann-Whitney rank sum test, $p < 0.05$ (*).

Figure 3: **Increased apoptosis in the spleen upon ABT-737 treatment.**

(A -C) *Il10*$^{-/-}$ mice suffering from spontaneous colitis. (A) Decreased number of CD8^{+} splenocytes in *Il10*$^{-/-}$ upon ABT-737 compared to vehicle determined by flow cytometry. Number of CD4^{+} and CD8^{+} splenocytes in *Bim*$^{-/-}$ x *Il10*$^{-/-}$ remained unchanged upon ABT-737. Statistical analysis was performed using the Mann-Whitney rank sum test, $p < 0.05$ (*). (B) Decreased number of CD8^{+} splenocytes in *Il10*$^{-/-}$ upon ABT-737 compared to vehicle determined by flow cytometry. (C) Mass cytometric analysis of TCRβ+ splenocytes revealed a significantly decreased proportion of CD3^{+} CD8^{+} T cells upon ABT-737 compared to vehicle. Statistical analysis was performed using the Holm-Sidak method, $p < 0.05$ (*).

Figure 4: **Increased number of TUNEL^{+} cells in Peyer's patches of the small bowel upon ABT-737.** (A) *Il10*$^{-/-}$ mice were sacrificed at day 14. Original magnification × 630. Statistical analysis was performed using the Mann-Whitney rank sum test, $p < 0.05$ (*). (B) The number of cells was calculated from four high power fields for each mouse. (C) Mass cytometric analysis of LPMNC revealed a significantly decrease in dead cells upon ABT-737 compared to vehicle. Statistical analysis was performed using the Holm-Sidak method, $p < 0.05$ (*). (D) Mass cytometric analysis of LPMNC revealed a decrease in both CD3^{+} CD4^{+} and CD3^{+} CD8^{+} T cells upon ABT-737 compared to vehicle.

Figure 5: **Mice suffering from colitis develop an ameliorated intestinal inflammation upon ABT-737-treatment as compared to vehicle-receiving mice.**

(A and B) *Il10*$^{-/-}$ mice suffering from spontaneous colitis. (A) Representative images demonstrate colonoscopy pictures derived from ABT-737- and vehicle-treated mice. (B) Statistical analysis of colonoscopy score (MEICS). Normality test was passed and statistical analysis was performed using One Way ANOVA (Bonferroni t-test). Colonoscopy was performed on the day prior to sacrificing the animals. Box plots express median, 95/5 % percentiles and outliers, $p < 0.05$ (*).

Figure 6: **ABT-737 treatment was followed by a significant increase of the colon length.**

(A - D) *Il10*$^{-/-}$ mice suffering from spontaneous colitis. (A) In *Il10*$^{-/-}$ mice ABT-737 treatment was followed by a significant increase in colon length. Statistical analysis was performed using the Mann-Whitney rank sum test. (B) Histological score was significantly decreased upon ABT-737 treatment. Statistical analysis was performed using the Mann-Whitney rank sum test. Box plots express median. (C) H&E staining of distal colon. Images representative for n = eight each, $p < 0.05$ (*),$p < 0.001$ (***). (D) Body weight curve.

Figure 7: **Significantly increased apoptosis in $CD4^+CD62L^+$ from *Il10*$^{-/-}$ mice upon ABT-737 pre-treatment as compared to vehicle.** (A) $CD4^+CD62L^+$ cells were isolated from *Il10*$^{-/-}$ mice treated for 14 days with ABT-737 or vehicle *in vivo*. $CD4^+CD62L^+$ cells were stimulated in vitro with ABT-737 or vehicle in a dose dependent manner. Following ABT-737 pre-treatment, cells became significantly more susceptible to the initiation of apoptosis as determined by flow cytometry. (B) *BIM* / *BCL-2* ratio was significantly decreased in $CD4^+CD62L^+$ from ABT-737-treated mice compared to vehicle treated mice. (C) *BCL-2* and *BCL-x*$_L$ qPCR of splenocytes isolated from *Il10*$^{-/-}$. Gene expression was increased in a time-dependent manner and upon ABT-737-treatment compared to vehicle-receiving controls. Statistical analysis was performed using the Mann-Whitney rank sum test, $p < 0.05$ (*).

Figure 8: **During long-term treatment *Il10*$^{-/-}$ mice develop intestinal inflammation despite ABT-737 application (50mg/kg/three days over 14 and 56 days), similarly to vehicle-receiving mice.** (A) Representative images demonstrate colonoscopy pictures derived from ABT-737- and vehicle-treated *Il10*$^{-/-}$ mice. (B) Statistical analysis of colonoscopy score (MEICS). Colonoscopy was performed on days 14 and 56, (one day prior to sacrificing the animals). Box plots express median, 95/5 % percentiles and outliers. (C) The cytokine profile of peripheral blood lymphocytes isolated from *Il10*$^{-/-}$ is altered in a time-dependent manner upon ABT-737-treatment compared to vehicle controls. *TNF* mRNA expression levels determined by qPCR. Statistical analysis was performed using the Mann-Whitney rank sum test, $p < 0.05$ (*).

Figure 1

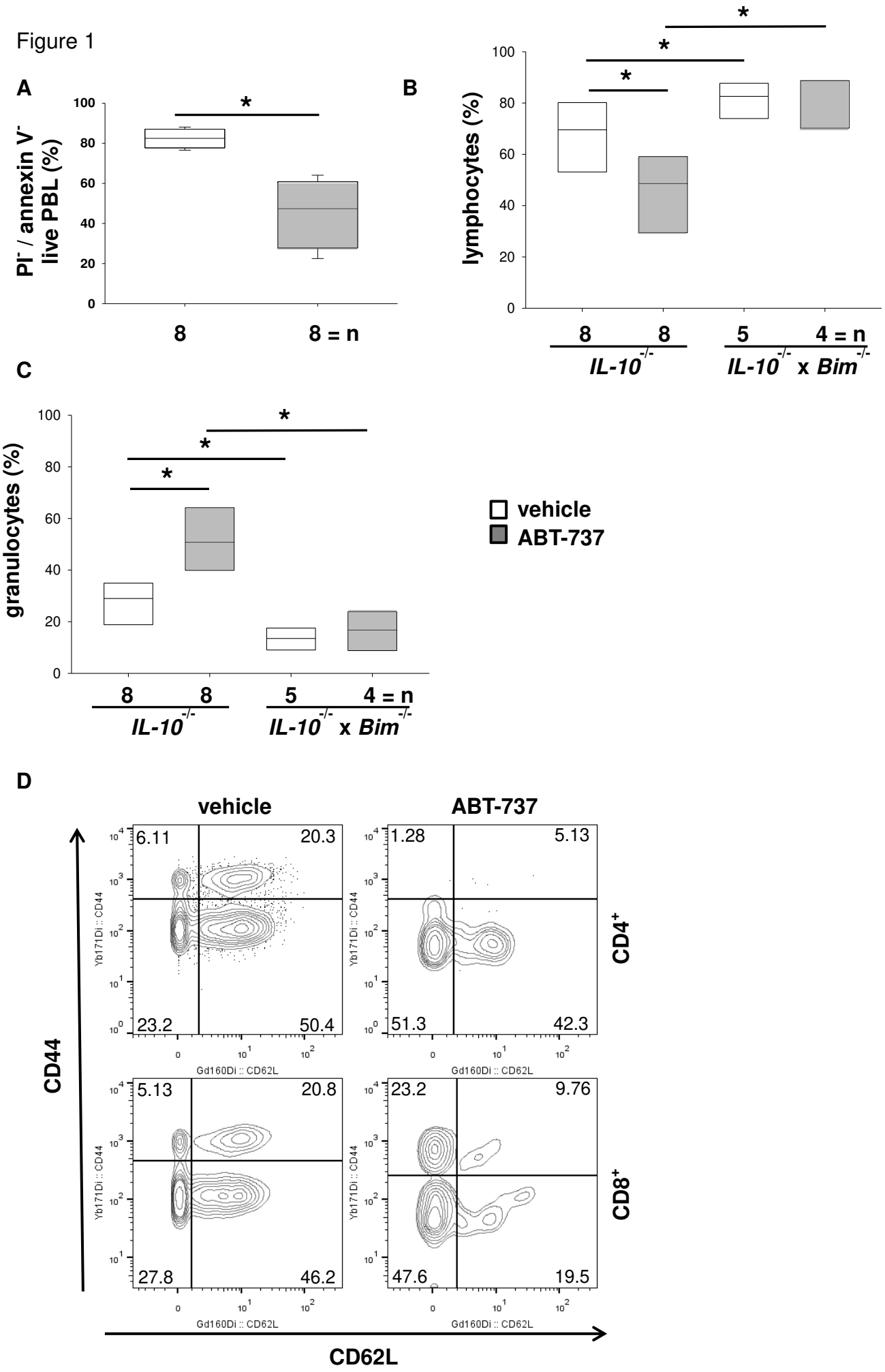
A
PI- / annexin V-
live PBL (%)
100
80
60
40
20
0
*
8
8 = n
B
lymphocytes (%)
100
80
60
40
20
0
*
*
*
8
8
5
4 = n
IL-10-/-
IL-10-/- x Bim-/-
C
granulocytes (%)
100
80
60
40
20
0
*
*
*
8
8
5
4 = n
IL-10-/-
IL-10-/- x Bim-/-
vehicle
ABT-737
D
vehicle
ABT-737
6.11
20.3
23.2
50.4
1.28
5.13
51.3
42.3
5.13
20.8
27.8
46.2
23.2
9.76
47.6
19.5
Yb171Di :: CD44
Gd160Di :: CD62L
CD4+
CD8+
CD44
CD62L

Figure 2

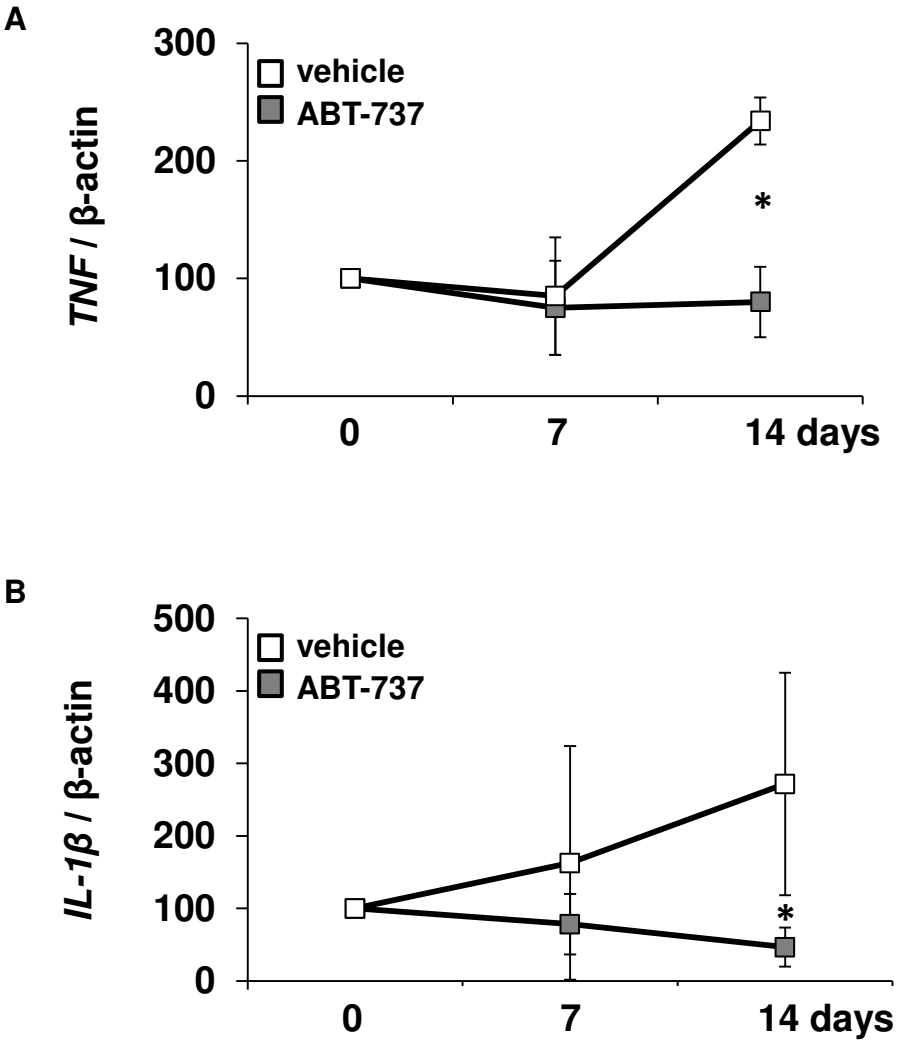
A
300
200
100
0
vehicle
ABT-737
TNF / β-actin
*
0
7
14 days
B
500
400
300
200
100
0
vehicle
ABT-737
IL-1β / β-actin
*
0
7
14 days

Figure 3:

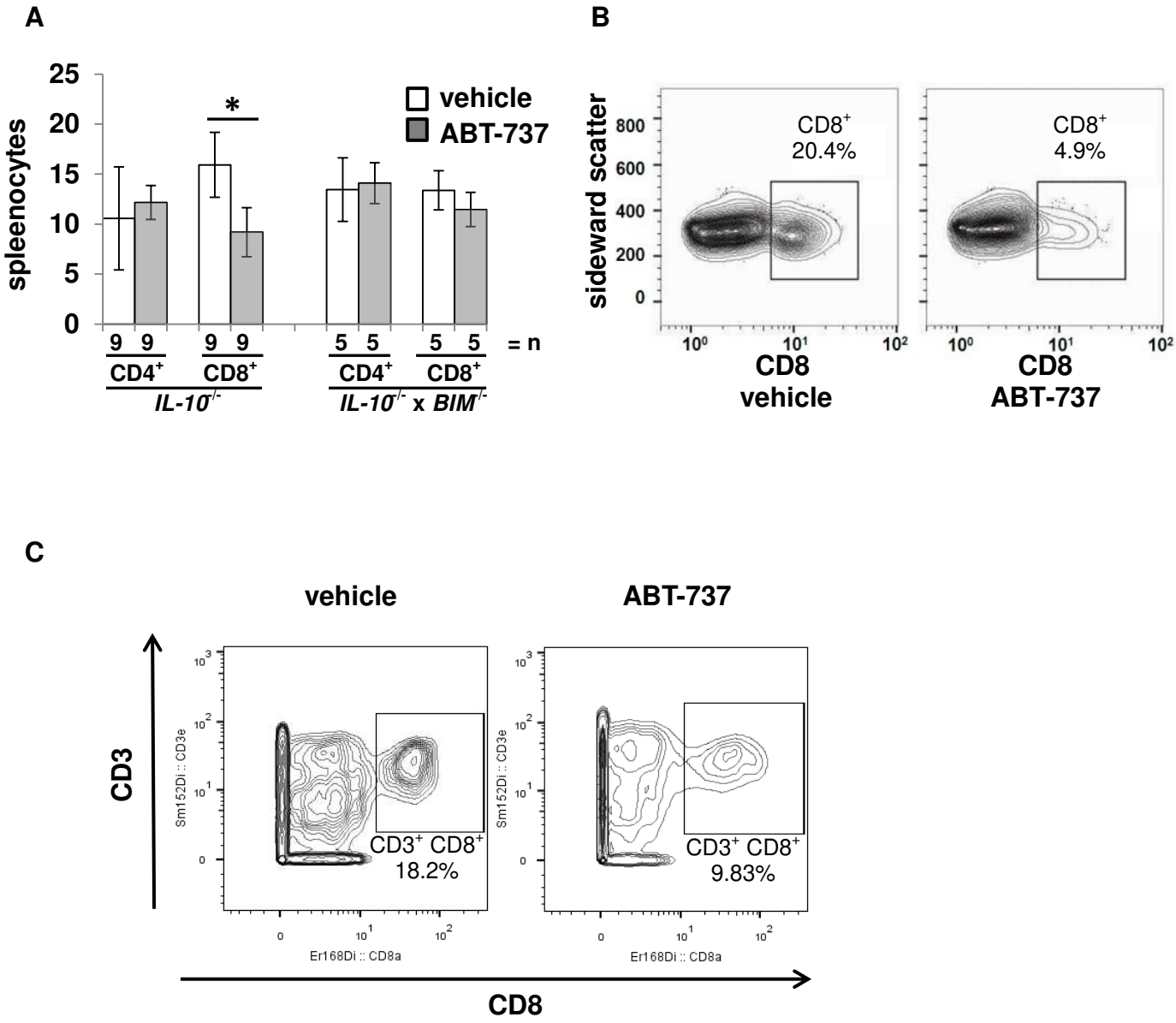
A
B
C
spleenocytes
vehicle
ABT-737
*
9 9 9 9 5 5 5 5 = n
CD4+ CD8+ CD4+ CD8+
IL-10-/-
IL-10-/- x BIM-/-
sideward scatter
CD8+ 20.4%
CD8+ 4.9%
CD8 vehicle
CD8 ABT-737
vehicle
ABT-737
CD3
CD8
Sm152Di :: CD3e
Er168Di :: CD8a
CD3+ CD8+ 18.2%
CD3+ CD8+ 9.83%

Figure 4:

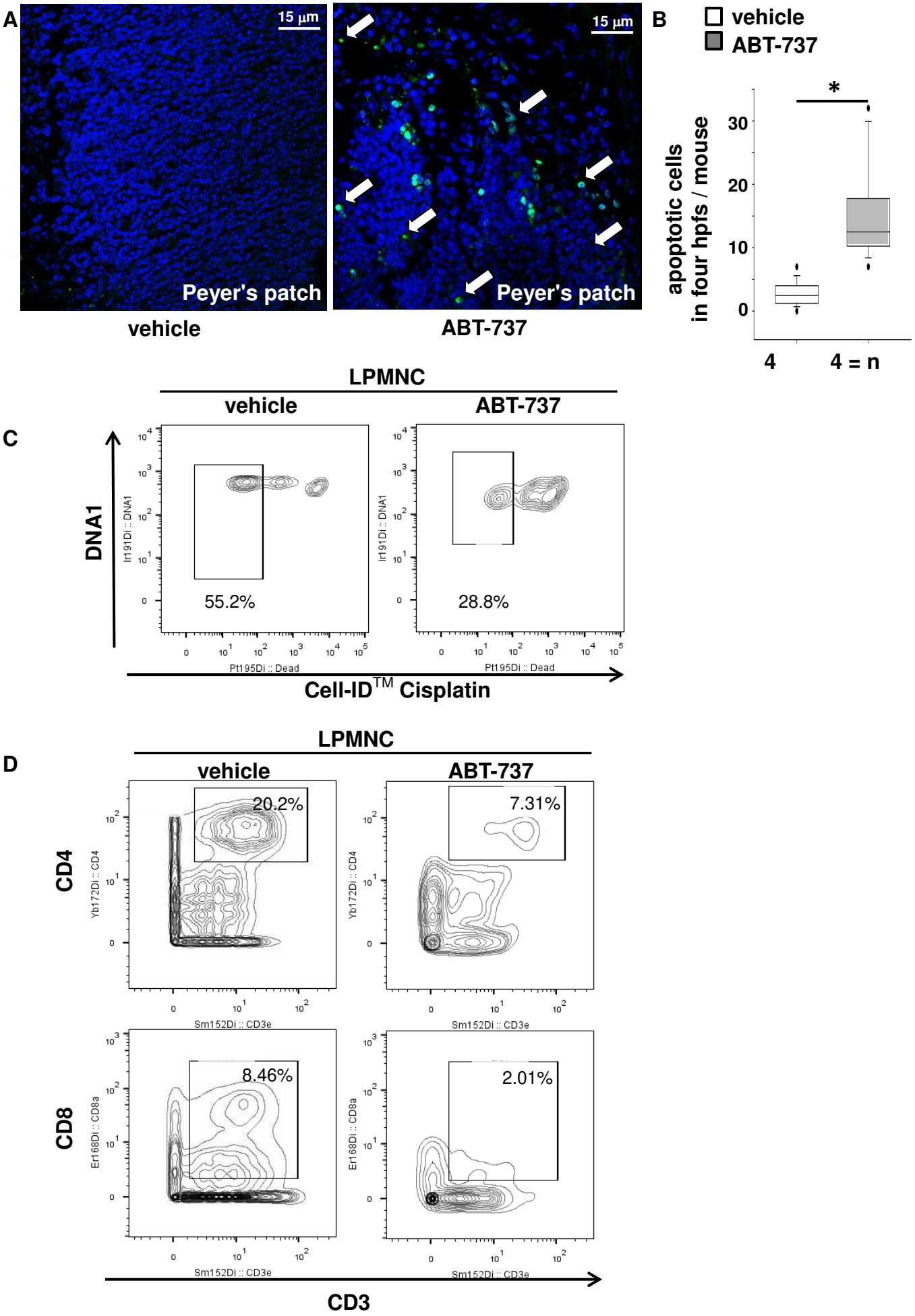
A
15 µm
Peyer's patch
vehicle
15 µm
Peyer's patch
ABT-737
B
vehicle
ABT-737
*
apoptotic cells in four hpfs / mouse
30
20
10
0
4
4 = n
C
LPMNC
vehicle
ABT-737
DNA1
Ir191Di :: DNA1
55.2%
28.8%
Pt195Di :: Dead
Cell-ID™ Cisplatin
D
LPMNC
vehicle
ABT-737
CD4
Yb172Di :: CD4
20.2%
7.31%
Sm152Di :: CD3e
CD8
Er168Di :: CD8a
8.46%
2.01%
CD3

Figure 5:

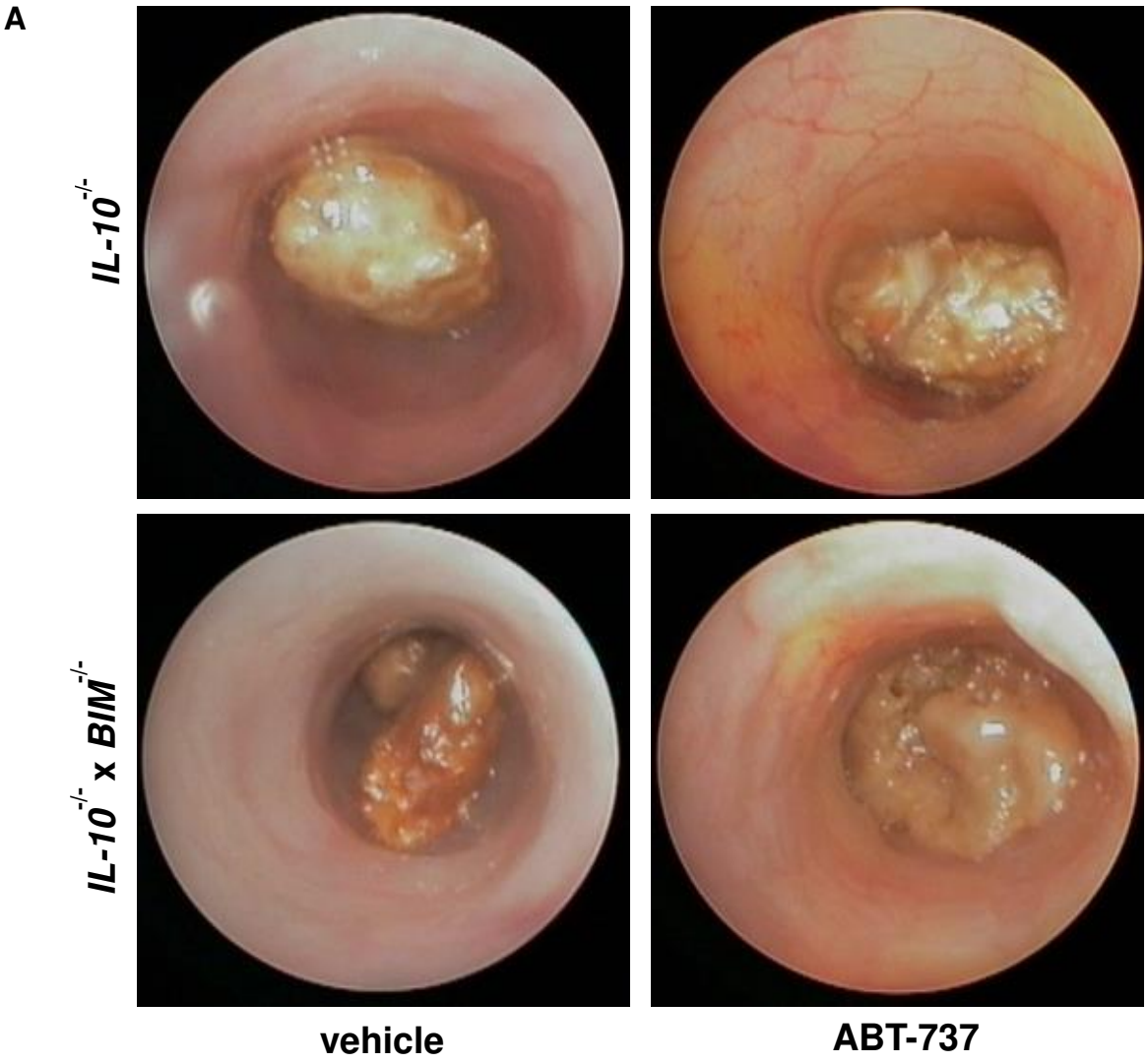
A
IL-10-/-
IL-10-/- x BIM-/-
vehicle
ABT-737
B
vehicle
ABT-737
MEICS
12
10
8
6
4
2
0
*
14
18
4
4 = n
IL-10-/-
IL-10-/- x BIM-/-

Figure 6

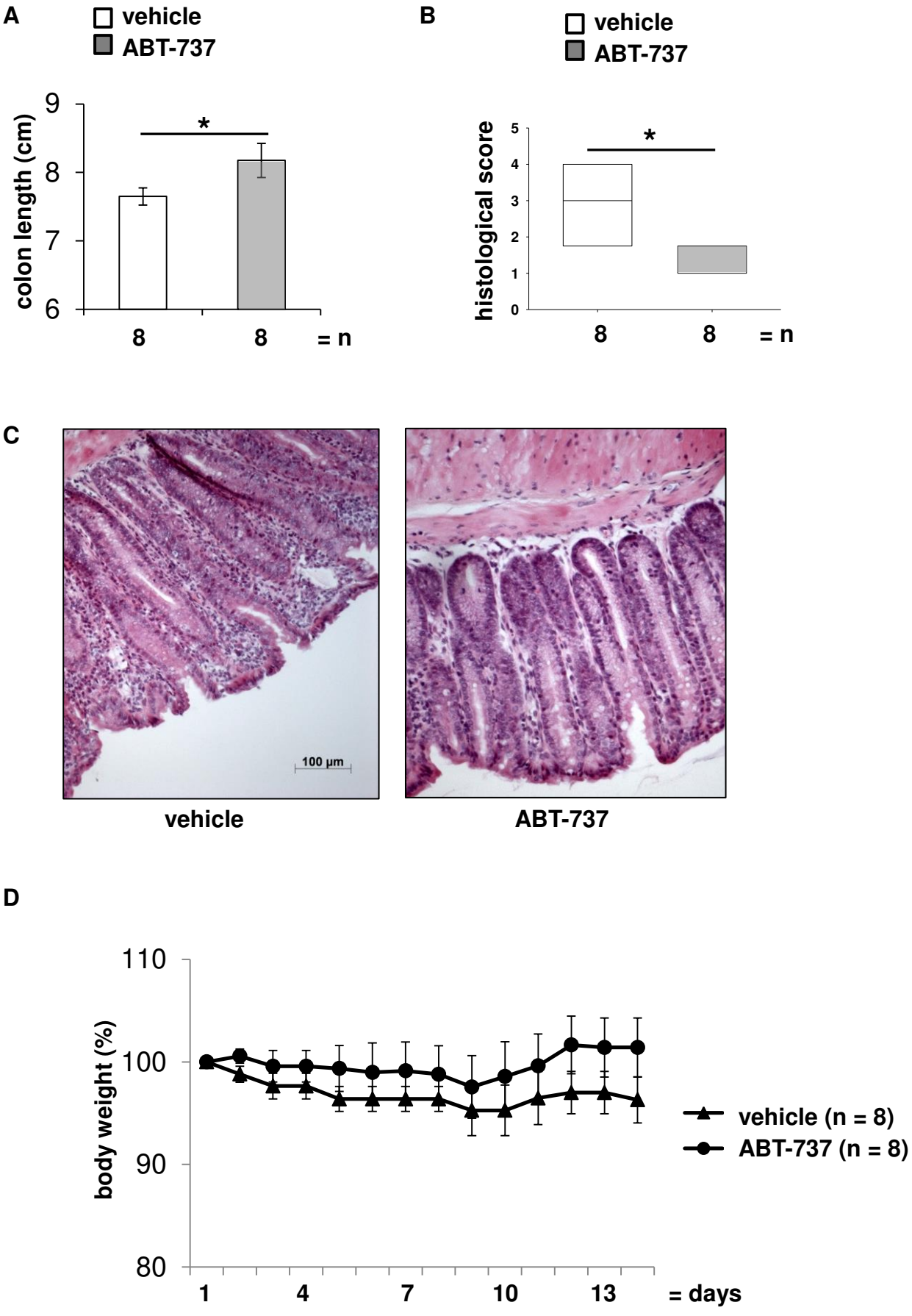
A
vehicle
ABT-737
colon length (cm)
9
8
7
6
*
8
8
= n
B
vehicle
ABT-737
histological score
5
4
3
2
1
0
*
8
8
= n
C
100 µm
vehicle
ABT-737
D
body weight (%)
110
100
90
80
1
4
7
10
13
= days
vehicle (n = 8)
ABT-737 (n = 8)

Figure 7:

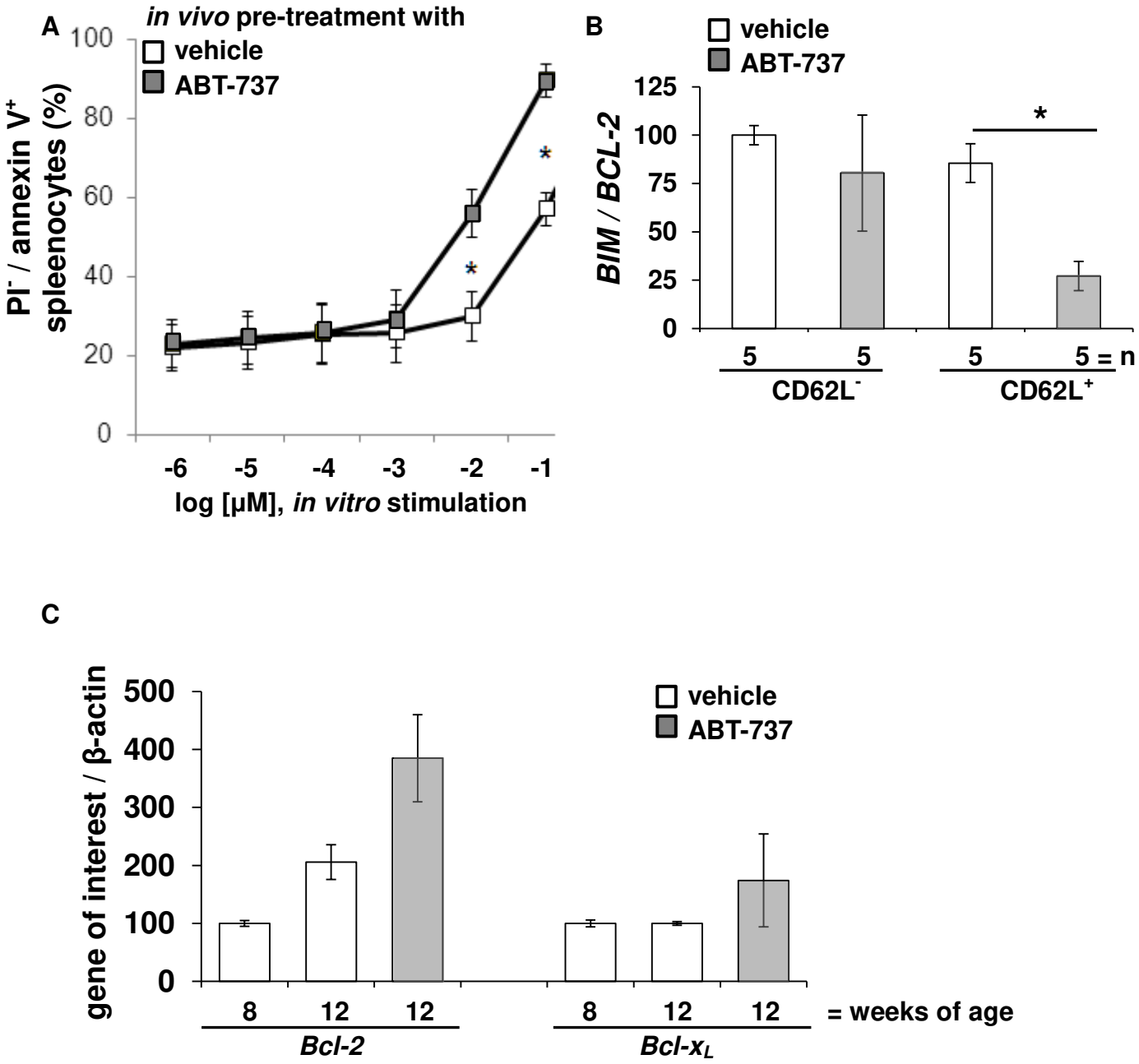
A
in vivo pre-treatment with
vehicle
ABT-737
PI- / annexin V+ spleenocytes (%)
100
80
60
40
20
0
-6
-5
-4
-3
-2
-1
log [µM], in vitro stimulation
*
*
B
vehicle
ABT-737
BIM / BCL-2
125
100
75
50
25
0
*
5
5
5
5 = n
CD62L-
CD62L+
C
gene of interest / β-actin
500
400
300
200
100
0
vehicle
ABT-737
8
12
12
8
12
12
= weeks of age
Bcl-2
Bcl-xL

Figure 8:

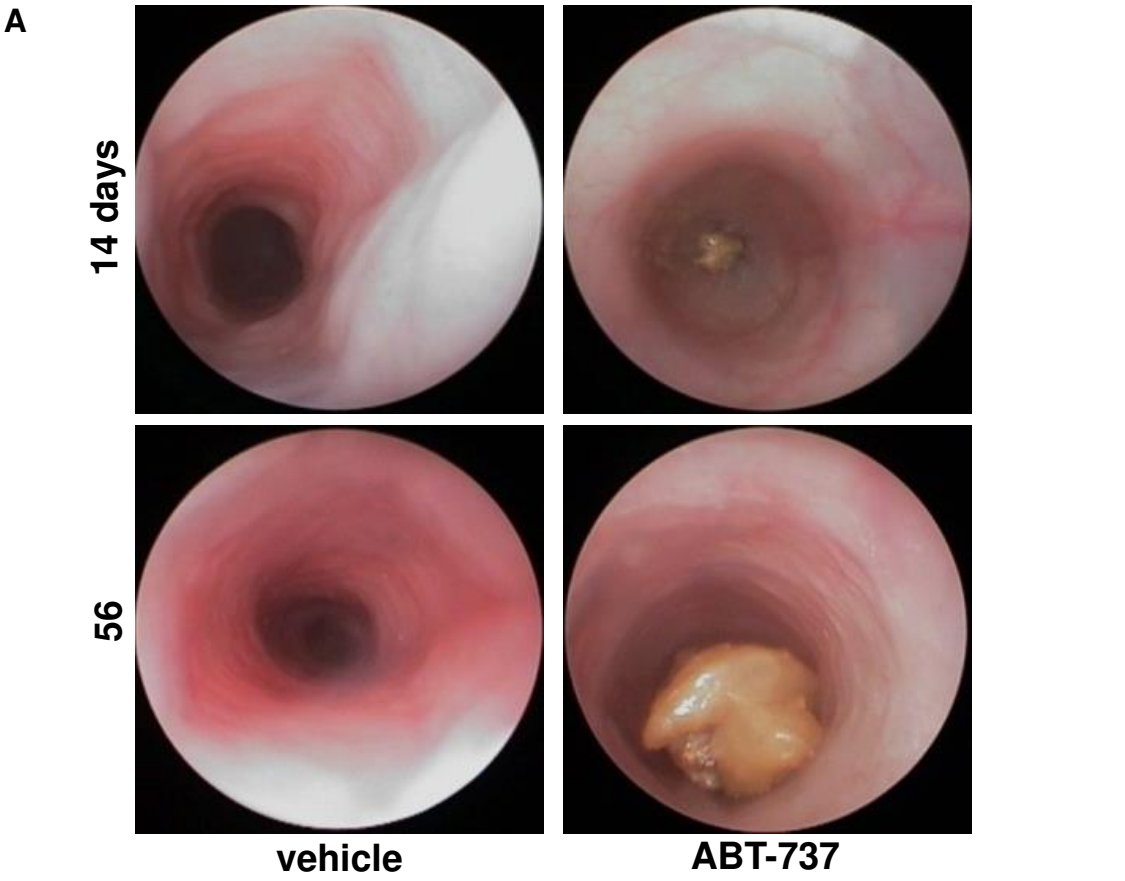
A
14 days
56
vehicle
ABT-737
B
MEICS
14
12
10
8
6
4
2
5
5
5
5 = n
14
56
days
vehicle
ABT-737
C
TNF / β-actin
5
4
3
2
1
*
10 9
9 9
9 9
9 9
10 9 = n
0
14
28
42
56
days
vehicle
ABT-737

Supplemental data

RESULTS

ABT-737 induces a significant lymphopenia in mouse models of colitis

Additionally hematological analyses for C57-BL/6J-Fue mice with a DSS-induced acute colitis were performed. After nine daily injections of ABT-737 a significantly reduced lymphocyte count was shown compared to controls ($1.48 \pm 0.98 \times 10^3$ cells/µL, $n = 10$ vs. $3.49 \pm 2.60 \times 10^3$ cells/µL, $n = 13$ respectively, $p < 0.05$, supplemental figure 1A). Similarly, ABT-737 mice had a significant reduction in thrombocytes ($485 \pm 141 \times 10^3$ platelets/µL, $n = 10$ vs. $837 \pm 233 \times 10^3$ platelets/µL, $n = 13$, $p < 0.05$). Accordingly a significantly increased fraction of combined granulocytes and monocytes in ABT-737 mice was found (34.3 ± 7.4 %, $n = 10$ vs. 20.8 ± 10.1 %, $n = 13$, $p < 0.05$, supplemental figure 1B). ABT-737 levels in peripheral blood determined by MS were directly correlated to the removal of lymphocytes, as well as the increased fractions of granulocytes and monocytes (supplemental figure 1C). Animals with high levels of ABT-737 displayed high efficacy in lymphocyte removal, while animals with minimal levels of ABT-737 had almost normal lymphocyte counts. The fraction of combined granulocytes and monocytes was inversely proportional to ABT-737 levels (supplemental figure 1C). In contrast erythrocytes were not affected upon ABT-737 treatment ($8.57 \pm 1.32 \times 10^{12}$ cells/L, $n = 10$ vs. $8.07 \pm 1.09 \times 10^{12}$ cells/µL, $n = 13$). In *Bim*$^{-/-}$ mice lymphocyte counts and fraction of combined granulocytes and monocytes were not significantly different upon ABT-737 (supplemental figure 1A and B). Flow cytometry of peripheral blood cells indicated that proportions of $CD4^+$ remained unchanged upon DSS-induced acute colitis and after nine daily injections of ABT-737 in C57-BL/6J-Fue mice (16.1 ± 7.9 %, $n = 11$ vs. vehicle-receiving controls: 18.4 ± 13.4 %, $n = 12$ respectively). $CD8^+$ appeared to be diminished upon ABT-737 treatment, although the differences were not significant (7.8 ± 3.2 %, $n = 10$ vs. 10.7 ± 6.2 %, $n = 12$ respectively). The fraction of autoreactive $CD4^+$ lymphocytes positive for TCR Vβ8 (46.8 ± 6.7 %, $n = 4$ vs. 46.2 ± 10.9 %, $n = 5$ respectively) and $CD8^+$ lymphocytes positive for TCR VB8 (45.3 ± 10.2 %, $n = 3$ vs. 39.0 ± 17.7 %, $n = 5$ respectively) remained unchanged.

Supplemental figure 1

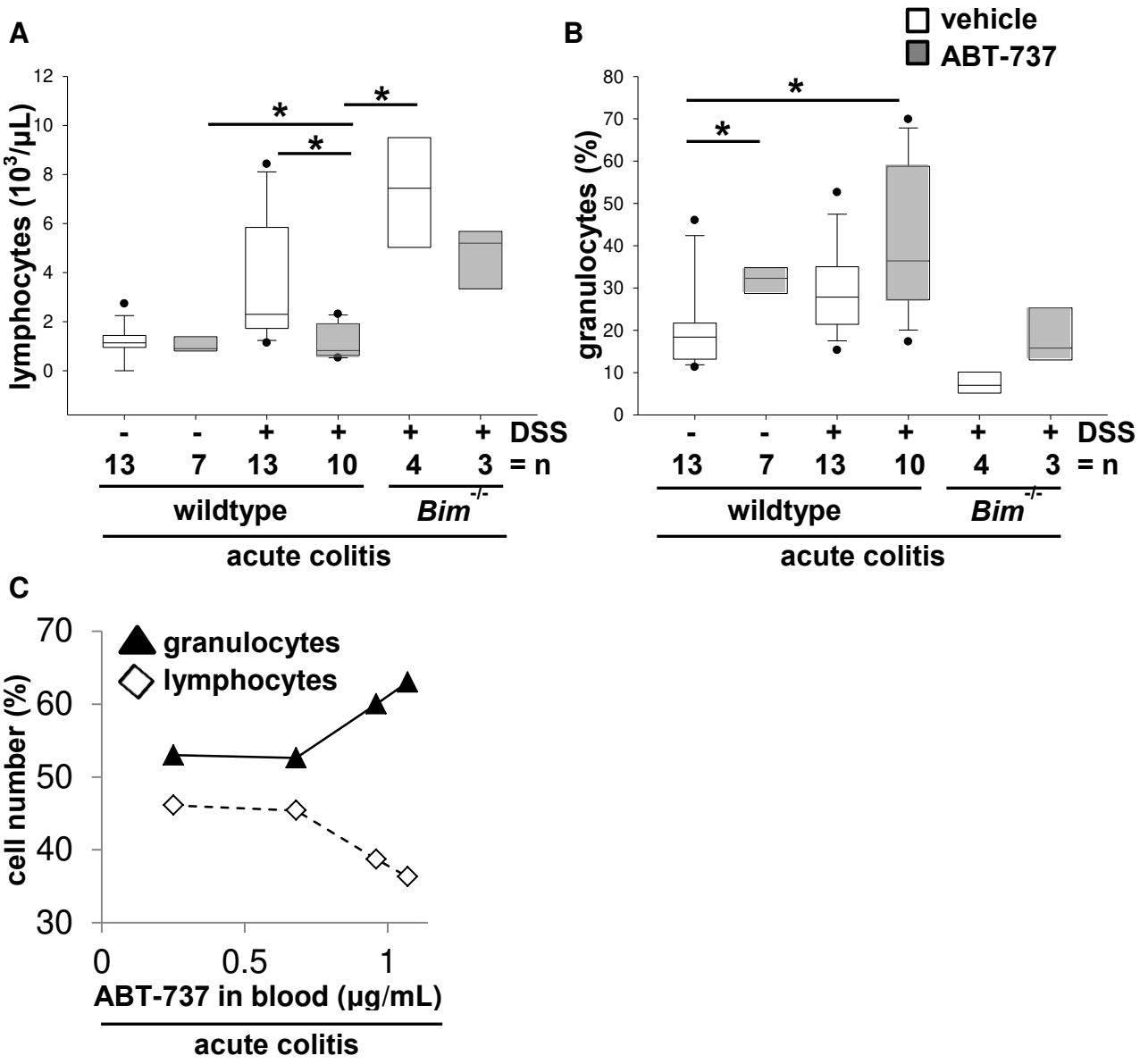

Supplemetal figure 1 **Cell death upon ABT-737 is selective for PBL**

(A - C) C57-BL/6J-Fue and *Bim*$^{-/-}$ mice upon DSS-induced acute colitis (vehicle = white, ABT-737 = grey). Hematological analyses revealed (A) a significantly decreased number of lymphocytes and (B) a significantly increased number of granulocytes upon ABT-737 compared to vehicle controls. ANOVA and Kruskal-Wallis One Way Analysis of Variance on Ranks (Dunn's Method). (C) ABT-737 levels were directly related to the removal of lymphocytes.

Supplemental figure 2

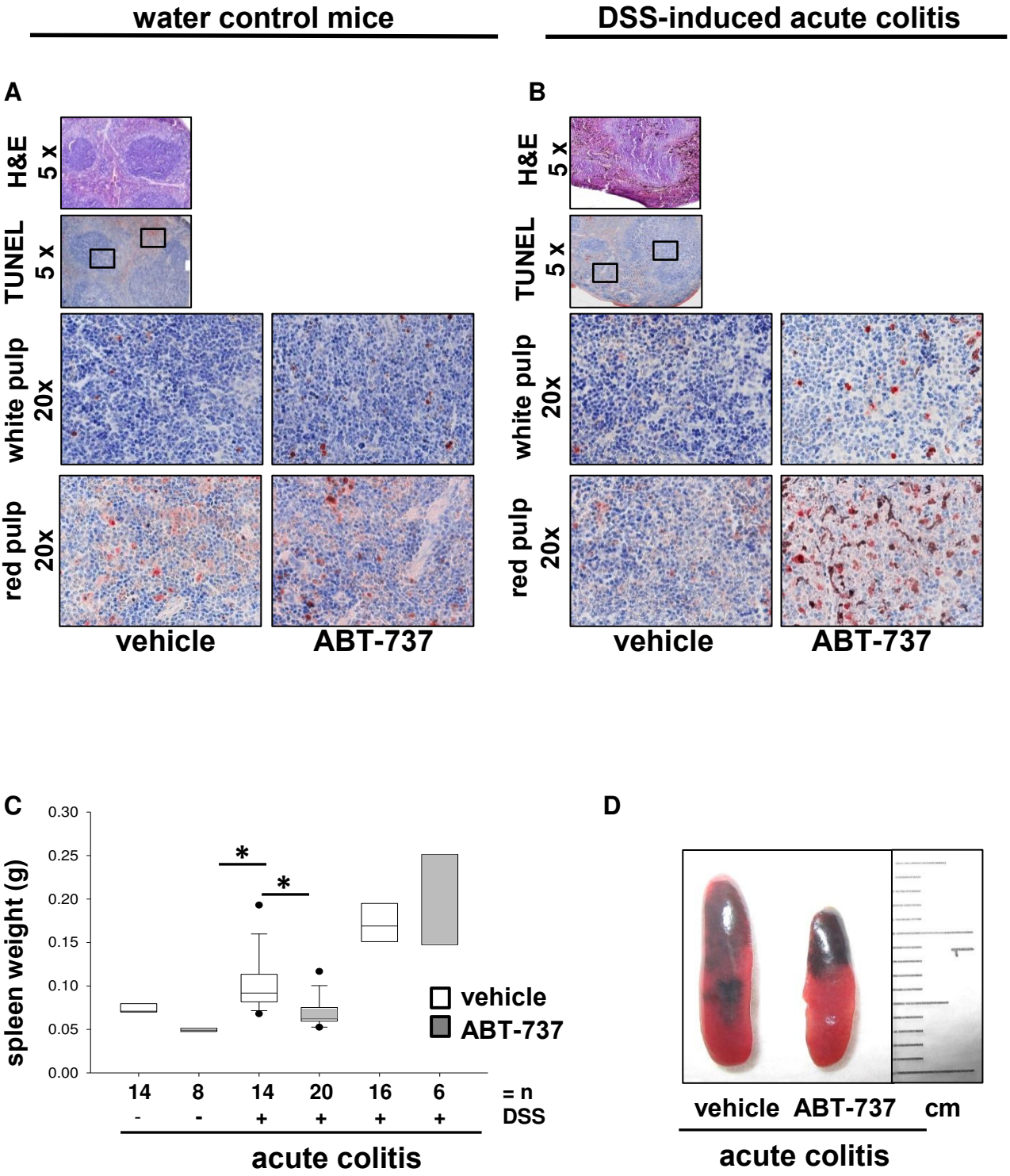

Supplemental figure 2: **Increased apoptosis in the spleen upon ABT-737 treatment.**

(A - D) C57BL/6 mice with DSS-induced acute colitis. (A) H&E staining and $TUNEL^+$ cells (red) in spleen upon ABT-737 treatment. Mice treated with ABT-737 or vehicle received either (A) water or (B) DSS. Mice were sacrificed at day nine. Treatment with ABT-737 was followed by an increase in $TUNEL^+$ cells in both red pulp and white pulp. Images representative for five mice each. Original magnification as indicated. (C) Spleen weights in DSS-induced acute colitis in C57BL/6 mice. C57BL/6 mice were treated with ABT-737 or vehicle and received either water or DSS. Treatment with ABT-737 was followed by a decrease in spleen weight. Induction of colitis was followed by a significant increase of the spleen, shown to be significantly decreased upon ABT-737. Statistical analysis was performed using the Kruskal-Wallis one way ANOVA, all pairwise multiple comparison procedures (Dunn's method), $p < 0.05$ (*). (D) Spleen of a mouse which received vehicle (left) or ABT-737 (right) upon DSS. Images representative for fourteen and twenty mice, respectively.

Supplemental figure 3:

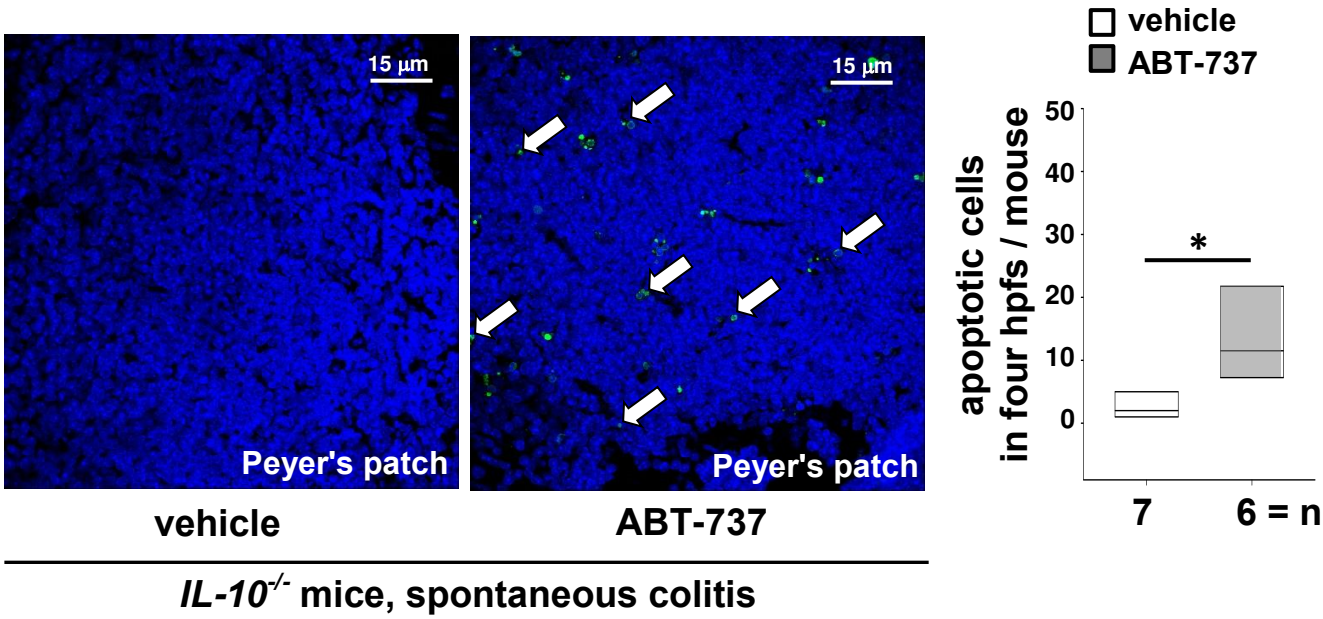

Supplemental figure 3: **Increased number of TUNEL$^+$ cells in Peyer's patches of the small bowel upon ABT-737 compared to vehicle treatment in the *IL-10*$^{-/-}$ model of spontaneous colitis.** Mice upon ABT-737 or vehicle were sacrificed at day five. Original magnification × 630. Statistical analysis was performed using the Mann-Whitney rank sum test, $p < 0.05$ (*). The number of cells was calculated from four high power fields for each mouse.

Supplemental figure 4

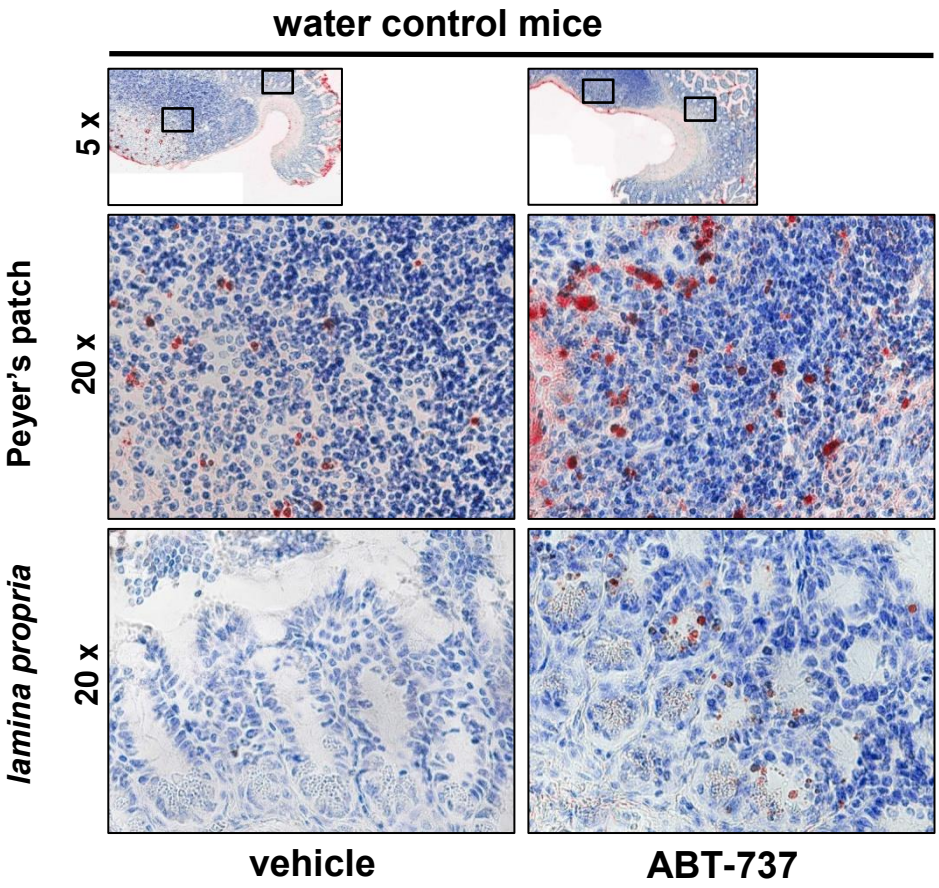

Supplemental figure 4: **Increased number of TUNEL$^+$ cells in Peyer's patches of the small bowel upon ABT-737.** Water control mice upon vehicle or ABT-737. Mice were sacrificed at day nine. Treatment with ABT-737 was followed by an increase in TUNEL$^+$ cells in Peyer's patches of the small bowel. Images representative for five mice each. Original magnification as indicated.

Supplemental figure 5:

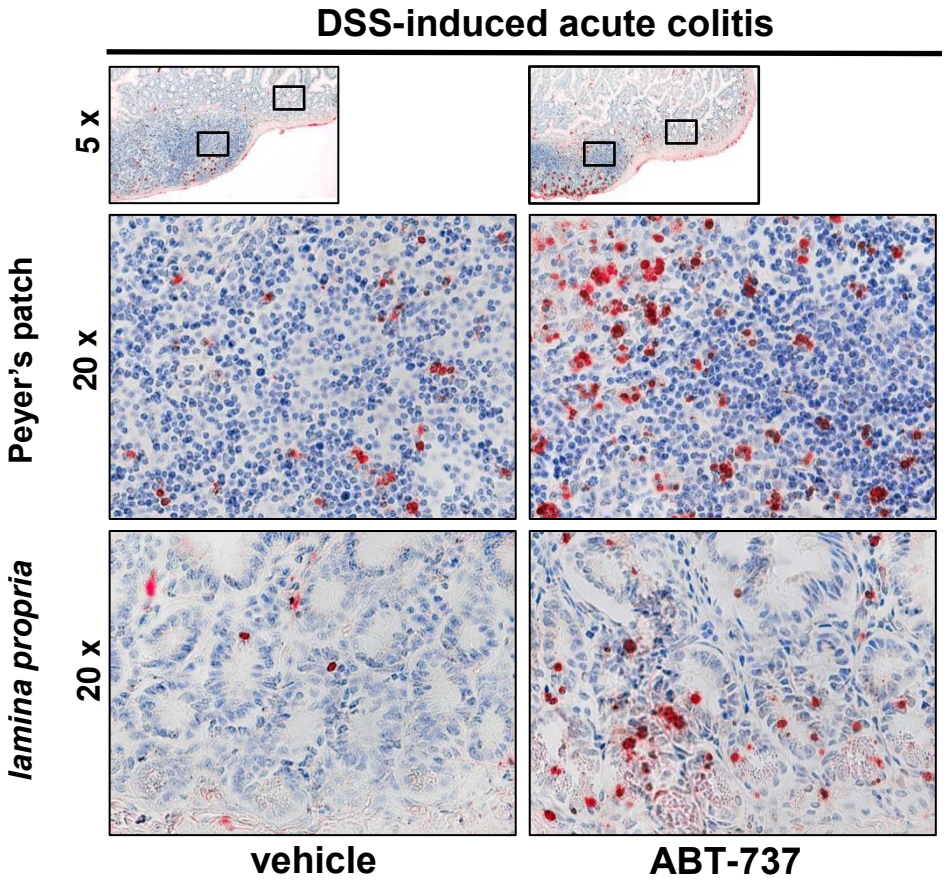

Supplemental figure 5: **Increased number of TUNEL$^+$ cells in Peyer's patches of the small bowel upon ABT-737.** Mice upon DSS were sacrificed at day nine. Treatment with ABT-737 was followed by an increase in TUNEL$^+$ cells in Peyer's patches. Images representative for five mice each. Original magnification as indicated.

Supplemental figure 6:

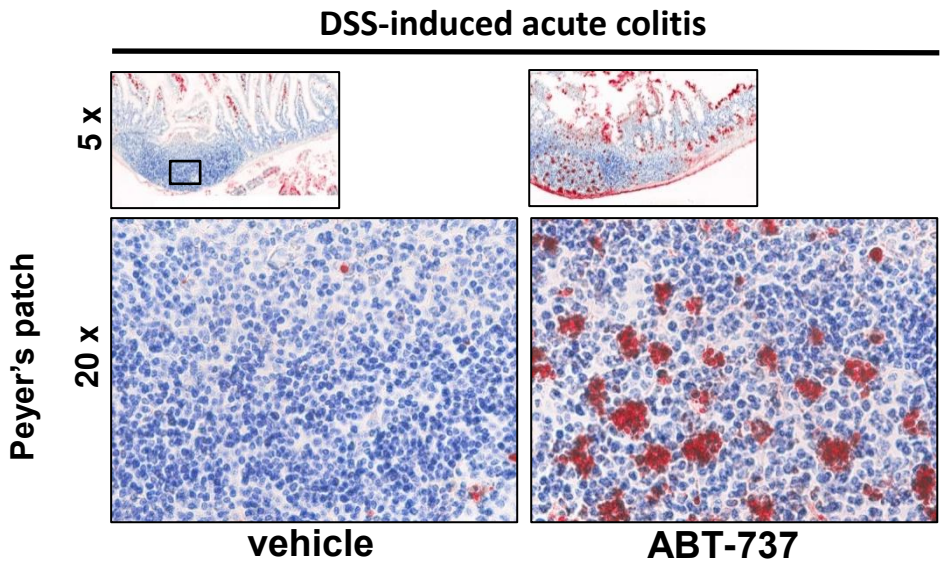

Supplemental figure 6: **Increased number of TUNEL$^+$ cells in Peyer's patches of the small bowel upon ABT-737 treatment in DSS-induced acute colitis in C57BL/6 mice.** TUNEL$^+$ cells frequently appeared as clusters of more than four cells in mice treated with ABT-737 compared to vehicle. Original magnification as indicated.

Supplemental figure 7

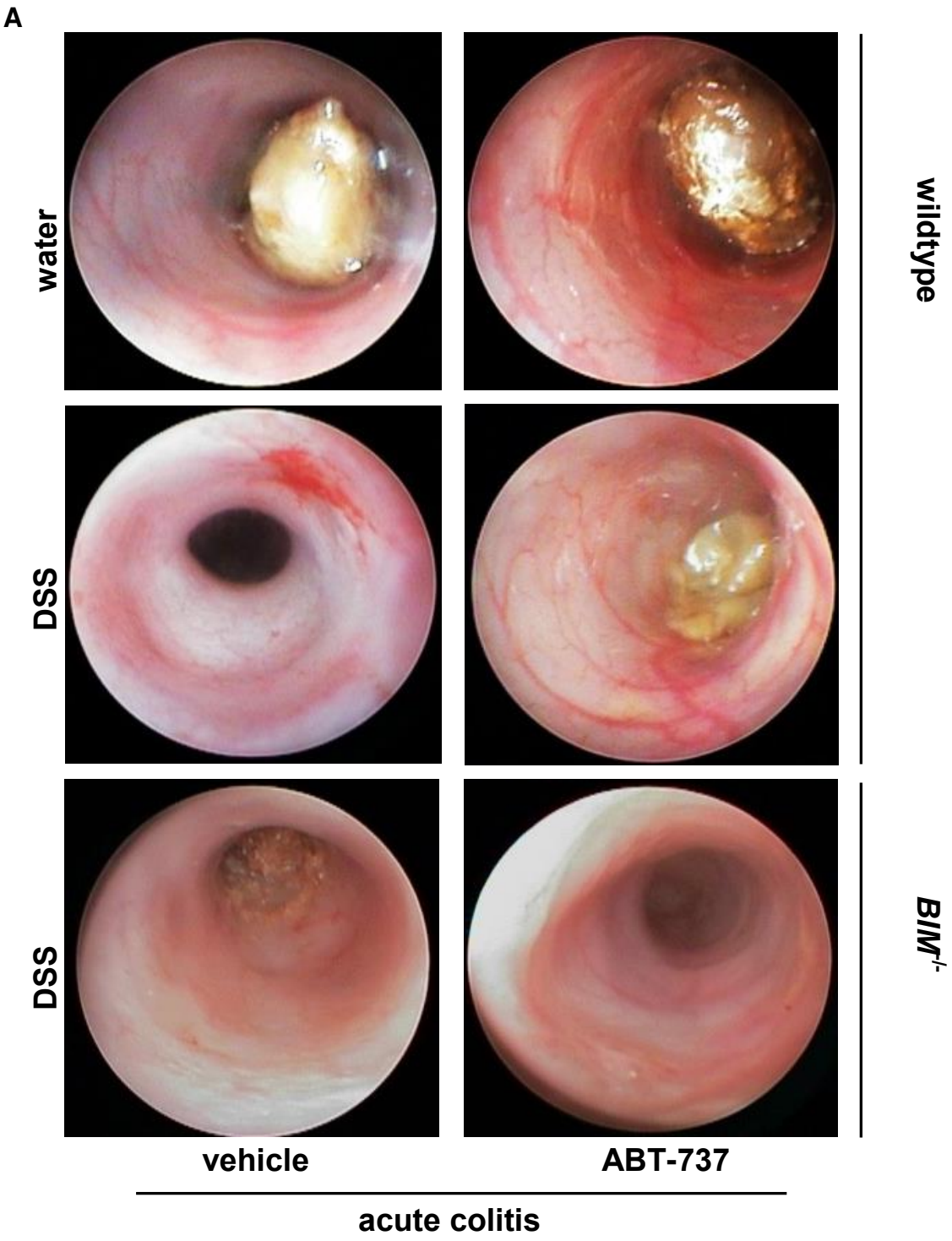

B

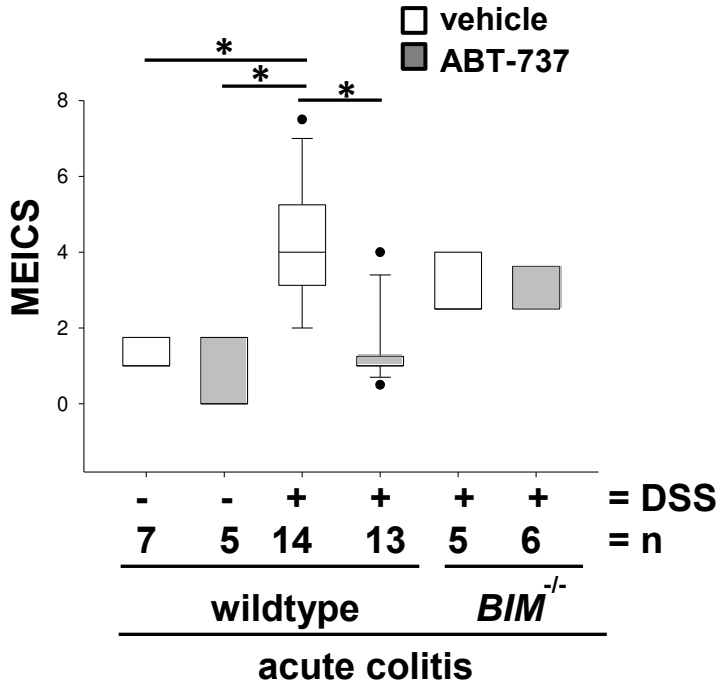

Supplemental figure 7: **Mice suffering from colitis develop an ameliorated intestinal inflammation upon ABT-737-treatment as compared to vehicle-receiving mice.** (A and B) C57BL/6 mice with DSS-induced acute colitis. (A) Representative images demonstrate colonoscopy pictures derived from ABT-737- and vehicle-treated mice. (B) Statistical analysis of colonoscopy score (MEICS). Statistical analysis was performed using the Kruskal-Wallis One Way Analysis of Variance on Ranks (Dunn's Method).

Supplemental figure 8

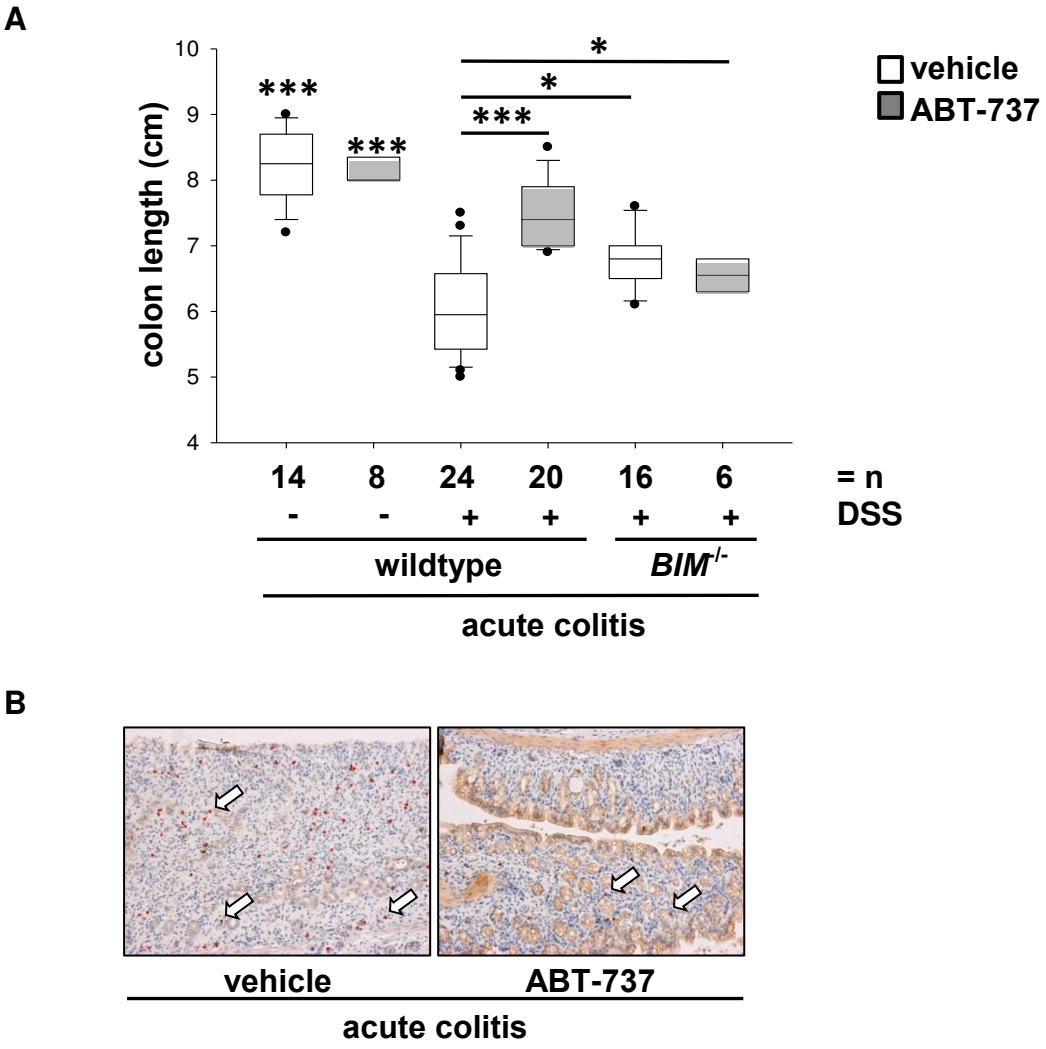

Supplemental figure 8: **ABT-737 treatment was followed by a significant increase of the colon length.** (A and B) Acute DSS- induced colitis in C57BL/6 mice. (A) Mice upon ABT-737 or vehicle received either water or DSS. Statistical analysis was performed using the one way ANOVA, all pairwise multiple comparison procedures (Bonferroni). (B) ABT-737-treatment was followed by a decrease in $CD3^+$ in colonic *lamina propria*. Original magnification x 10.

Supplemental figure 9

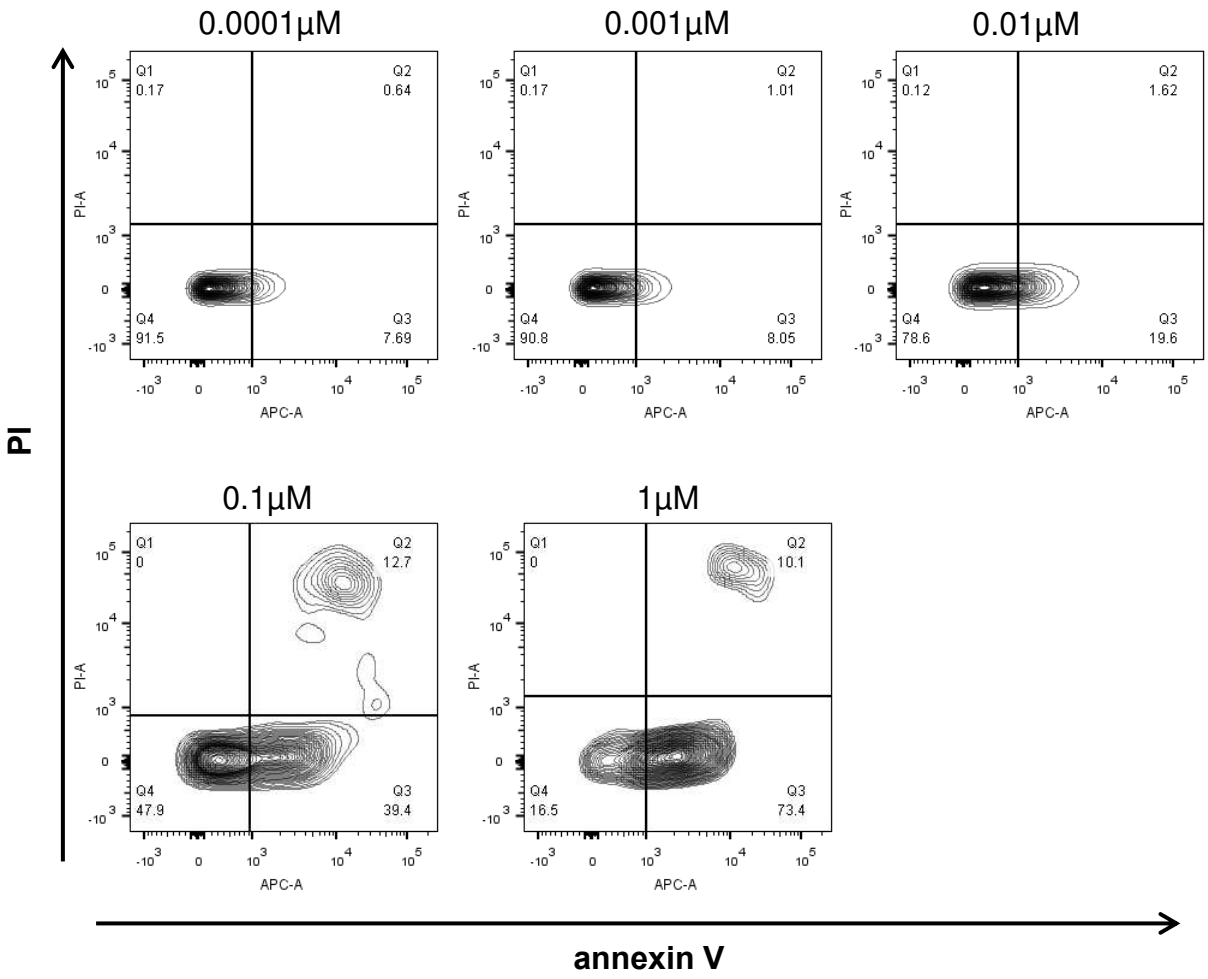

Supplemental figure 9: **ABT-737 treatment was followed by a significant increase of apoptosis in CD4$^+$CD62L$^+$ in a dose-dependent manner.** Contour plots. Following ABT-737 *in vivo* pre-treatment CD4$^+$CD62L$^+$ cells became susceptible to apoptosis initiated by ABT-737 compared to vehicle controls (ABT-737 concentration as indicated). Living cells, annexin V$^-$ / PI$^-$; apoptotic cells, annexin V$^+$ / PI$^-$.

Supplemental figure 10

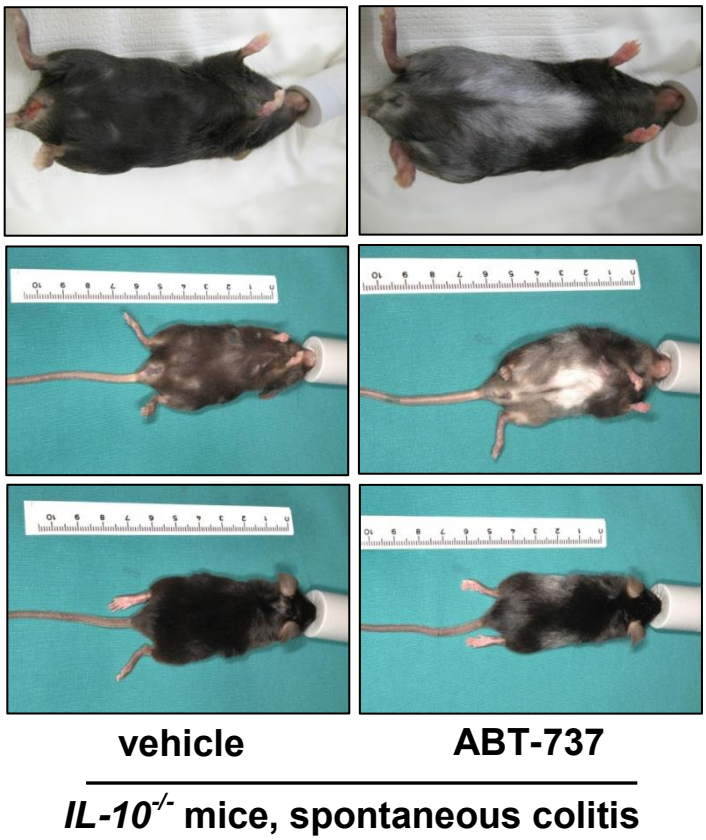

Supplemental figure 10: **Depigmentation of the abdominal fur.** Hair depigmentation after 56 days of long term treatment of *IL-10*$^{-/-}$ with ABT-737 (50 mg/kg/three days).